UNIVERSIDADE D
COIMBRA

Maria Inês de Sá Ribeiro

DYNAMICS OF MOTOR MEMORY CONSOLIDATION IN THE CEREBELLUM

Dissertação no âmbito do Mestrado em Biologia Celular e Molecular, com especialização em Neurobiologia orientada pela Doutora Megan Carey, com orientação interna do Professor Doutor João Peça e apresentada ao Departamento das Ciências da Vida da Faculdade de Ciências e Tecnologias da Universidade de Coimbra

Novembro de 2021

Agradecimentos / Acknowledgements

I would like to thank Dr. Megan Carey for the great feedback and for giving her perspective on the project, but most of all for the opportunity to work and learn in her lab. I would also like to thank everyone in the lab, not only for the thoughtful comments but also for their involvement, incredible spirit and friendship. A special thanks to Tatiana whose work I have given my collaboration, for all her support, patience and good advice. Also thank you to Merit for being so uplifting and making my caveman days fun. To the ”carey gang”, thank you for the fun (well deserved) nights out, making the most out of the world’s situation.

Mais do que tudo, quero agradecer à minha família a quem dedico todo o meu trabalho. Aos meus pais pelo suporte e amor incondicinal, por sempre acreditarem em mim mais do que ninguém. À minha irmã por ser a minha luzinha, pela cumplicidade e toda a galhofa. À minha querida avó por todo carinho e conversas do fundo do coração. To my dutch grandparents for being supportive and cheering all my conquers. Um obrigado especial à Ana, porque não interessa a distância, está sempre lá.

To all of you, I am very grateful.

Author Contributions

The work presented in this dissertation has been built from previous experiments done by Tatiana Silva, as part of her PhD thesis. For the past year, I have given a continuation of her work, doing part of the optogenetic experiments, as well as control experiments for the running activity during the reversible inactivation of the cerebellar cortex and preliminary experiments for the reversible inactivation of the cerebellar nuclei. Nonetheless, with her permission, all the data was included here to present the full story and rationale for the project.

With this, I deeply thank Tatiana for bringing me into her project and letting me give my collaboration.

Abstract

Motor learning is a crucial process that is present throughout life. Similar to declarative memories, motor memories also undergo consolidation over time, becoming less susceptible to interference. Despite its ubiquity, mechanisms for motor memory consolidation are still poorly understood. The cerebellum is essential for several forms of motor learning, including delay eyeblink conditioning, a form of associative learning. This learning task has been relevant to study how cellular activity contributes to motor memory consolidation. Here we investigated the dynamics of motor memory consolidation of eyeblink learned responses.

We have found that as the engagement in locomotor activity enhances the acquisition and expression of eyeblink conditioning responses, it also accelerates the consolidation of these memories. Only animals that were not actively locomoting during training sessions were susceptible to pharmacological and optogenetic perturbations of activity in the cerebellar cortex immediately after each training session. In contrast, post-session manipulations of neural activity had no effect on memory consolidation in mice that were trained on a motorized running wheel. Conversely, optogenetic perturbation of cerebellar granule cells in between the learning trials, impaired learning only in animals that were engaged in locomotion during training, but did not yield an effect in animals voluntarily locomoting during the task.

These results indicate a temporal discrepancy of the motor memory consolidation time window depending on locomotor engagement during task performance, suggesting that locomotion drives a shift in the critical time window for motor memory consolidation in the cerebellar cortex, from immediately following, to within training sessions. Further preliminary data suggest that running modulation may also promote a subtle earlier shift in memory storage location, from the cerebellar cortex to the cerebellar nuclei. Finally, our results also highlight the importance of the neuronal activity in the cerebellar cortex for the consolidation of eyeblink learned responses in mice.

Key words: Cerebellum; Eyeblink Conditioning; Motor Memory Consolidation

Resumo

A aprendizagem motora é um processo imprescindível que nos acompanha ao longo da vida. Tal como as memórias declarativas, memórias motoras também passam por um processo de consolidação ao longo do tempo que as torna menos suscetíveis a interferências. Apesar de ser um processo comum, os mecanismos subjacentes à consolidação de memórias motoras ainda não são completamente compreendidos.

O cerebelo é essencial para várias formas de aprendizagem motora, incluindo *eyeblink conditioning*, uma forma de aprendizagem associativa. Esta tarefa dependente do cerebelo tem sido relevante para estudar como a atividade neuronal contribui para a consolidação de memórias motoras. Neste projeto, o nosso objetivo foi investigar a dinâmica do processo de consolidação das memórias motoras associadas às respostas de *eyeblink conditioning*.

Os nossos resultados sugerem que, tal como acontece com a aquisição e expressão de respostas de *eyeblink conditioning*, a atividade locomotora acelera a consolidação dessas memórias. Apenas murganhos que não estavam ativamente em locomoção durante a sessão eram suscetíveis a perturbações farmacológicas e optogenéticas do córtex cerebelar feitas imediatamente após cada sessão de treino. Em contraste, as manipulações da atividade neuronal pós-sessão não tiveram efeito na consolidação destas memórias quando os animais eram treinados numa roda motorizada que faz com que se locomovam constantemente. Por outro lado, a perturbação optogenética de *granule cells* cerebelares entre cada *trial* das sessões de treino atrasou a aprendizagem apenas em animais que estavam ativamente a correr durante a sessão. A mesma perturbação optogenética não produziu um efeito em animais que estavam voluntariamente a andar durante a tarefa.

Estes resultados indicam uma discrepância temporal do período crítico da consolidação de memórias motoras, dependendo do envolvimento ativo em locomoção durante a tarefa. Sugerindo assim que correr leva a uma mudança na janela de tempo crítica para a consolidação da memória motora no córtex cerebelar, de imediatamente após, para durante as sessões de treino.

Resultados preliminares sugerem também que a corrida ativa durante a sessão de treino pode promover uma mudança do local de armazenamento das memórias de *eyeblink conditioning* do córtex para os núcleos cerebelares. Finalmente, os nossos resultados destacam a importância da atividade neuronal do córtex cerebelar na consolidação das memórias associadas a *eyeblink conditioning* em murganhos.

Palavras-chave:Cerebelo; Eyeblink Conditioning; Consolidação de Memórias Motoras

Índice

List of Figures

List of Abbreviations

AIP, anterior interpositus nucleus

ArchT, archaerhodopsin-3

CF, climbing fiber

ChR2, channelrhodopsin-2

CR, conditioned response

CS, conditioned stimulus

CTL, littermate control

DCN, deep cerebellar nuclei

GC-ArchT, Gabra6cre-ArchT

GC, granule cell

GC-ChR2, Gabra6cre-ChR2

GFP, green fluorescent protein

ITI, intertrial interval

ISI, interstimulus interval

LTD, long-term depression

MF, mossy fiber

MLIs, molecular layer interneurons

PC, Purkinje cell

PF, parallel fiber

US, unconditioned stimulus

WT, wild-type

YFP, yellow fluorescent protein

Chapter 1

Introduction

1.1 Motor Learning and Memory

The cerebellum was initially associated solely with motor control and coordination, a concept that arose from Flourens' studies in the early 1800s (Flourens, 1824). The knowledge of cerebellar functions has been largely driven by the effects of dysfunctions and lesions, and is strongly associated with disturbances in movement (Schmahmann, 1991).

This view changed in the 1960s through electrophysiological and morphological studies in John Eccles' laboratory, which first described the cellular structure of the cerebellar cortex (Eccles et al., 1967). Following this work, David Marr (Marr, 1969) and James Albus (Albus, 1971) proposed an influential theory, subsequently developed by Masao Ito (Ito, 1972), establishing a new role of the cerebellum. According to their work, the cerebellum is a site of motor learning, receiving divergent-convergent inputs to modulate motor output. In fact, recent studies have found that the cerebellum plays a role not only in motor but also in non-motor functions (Baumann et al., 2015; Schmahmann et al., 2019).

Interestingly, the cerebellum appears to have a modulatory role in movement. It acts as a "time and learning machine" by detecting errors and predicting the consequences of the actions. It then compares the actual outcome to then generate corrective signals (Ito, 2008; D'Angelo, Casali, 2013; Therrien, Bastian, 2019). This theory of cerebellar motor learning has been supported by several studies of classical eyeblink conditioning (Raymond et al., 1996).

1.2 Eyeblink Conditioning

Classical eyeblink conditioning is a simple cerebellum-dependent form of Pavlovian associative learning that aids the better adaptation of the subjects' future behavior to their environment (Rescorla, 1988; Medina et al., 2000b).

Various experiments have revealed the cerebellum dependence of eyeblink conditioning (McCormick, Thompson, 1984; Yeo et al., 1984; Krupa et al., 1993; Perrett et al., 1993; Garcia et al., 1999; Heiney et al., 2014). Through these studies, it was possible to identify the lobule IV/V of the cerebellar cortex as the required region for the acquisition and expression of eyeblink conditioning responses (Garcia et al., 1999; Heiney et al., 2014) and the anterior interpositus nucleus (AIP) as the critical region of the deep cerebellar nuclei (DCN) for this process (Krupa et al., 1993; Heiney et al., 2014). Overall, it has been found that learning occurs in both the cerebellar cortex and nucleus, even though this remains a topic of controversy (Lisberger, 2021).

1.2.1 Paradigm

Eyeblink conditioning consists of repeated pairing of a neutral conditioned stimulus (CS), such as a light (light CS), with an unconditioned stimulus (US), such as an air puff (air puff US) that reliably elicits blinking (Figure 1.1 A, B). This specific type of learning involves a gradual development of conditioned responses (CRs), that consist of blinking to the CS, in an accurately timed manner so that it occurs briefly before the US (Figure 1.1 C), (Medina et al., 2000b; De Zeeuw, Yeo, 2005). The CS can be a wide range of stimuli, including visual, auditory or tactile (De Zeeuw, Yeo, 2005). Eyeblink conditioning entails two main hallmarks: gradual CR acquisition (Figure 1.1 D) and adaptive timing of the learned responses.

There are two variants of eyeblink conditioning: delay and trace. In the delay, the light CS precedes the air puff US onset by a fixed interval (InterStimulus Interval – ISI) and the stimuli co-terminate, briefly overlapping. Whereas in the trace conditioning the light CS is followed by a period of no stimulation before the air puff US onset (Thompson, Steinmetz, 2009). The trace paradigm has been shown to involve other areas, such as the hippocampus and the frontal cortex (Kalmbach et al., 2010). In this thesis, I will refer to the delay paradigm as eyeblink conditioning, as that was the task selected to investigate motor-specific memory consolidation.

For learning of eyeblink conditioning to occur, the light CS must precede the air puff US by

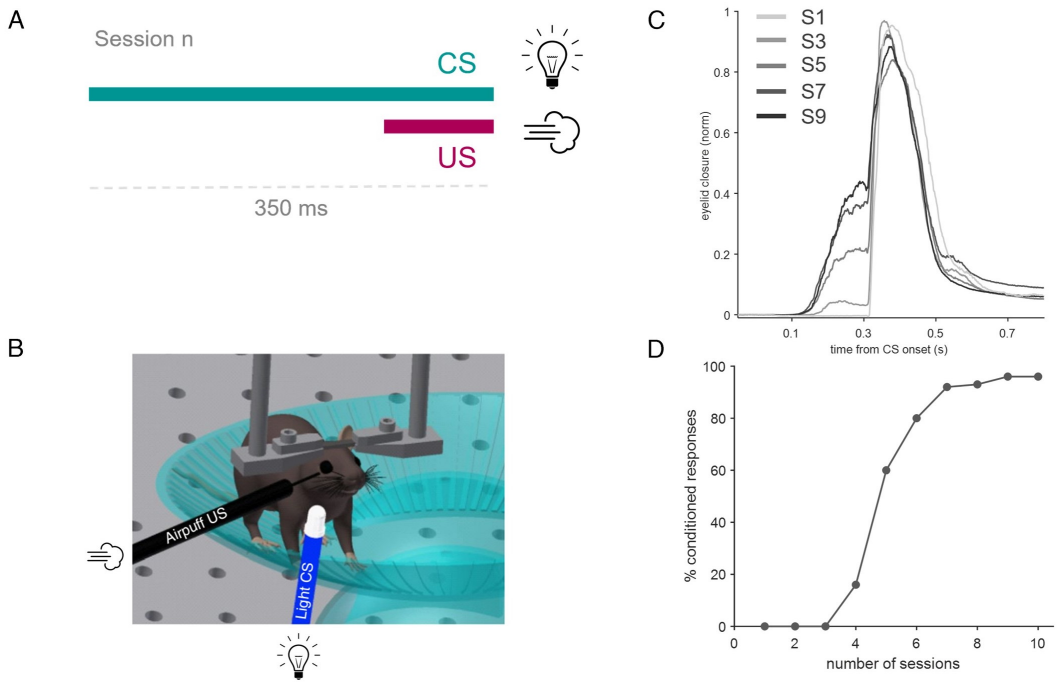

Figure 1.1: Features of delay eyelid conditioning. **A)** Schematic representation of CS-US pairing in delay eyeblink conditioning. **B)** Experimental apparatus with head-fixed mouse. Adapted from Albergaria et al. (2018) **C)** Average eyelid closure for a representative animal across 9 learning sessions, showing the gradual acquisition of CRs, which can be converted into a learning curve on a function of %CR over the learning sessions **D)**.

at least 100 ms and learning appears to worsen after 500 ms of ISI (Smith, 1968; Smith et al., 1969). The CR timing is adaptable to the used ISI so that the maximum eyelid closure occurs at the expected air puff US onset (Mauk, Ruiz, 1992; Chettih et al., 2011). Unconventionally, the cerebellar cortex accomplishes appropriately timed CRs not only by learning to act but also by learning to suppress acting both at the right time. In fact, the generation of a CR is driven by a response-suppression mediated by a learned pause in Purkinje cell (PC) activity, which, by disinhibiting the DCN, initiates movement (Medina et al., 2000a).

1.2.2 Circuits Within

Eyeblink conditioning, alongside other Pavlovian learning tasks such as fear conditioning, has been helpful to elucidate the neural circuits and anatomical areas relevant for motor memory and learning (Medina et al., 2000b, 2002).

1.2.2.1 Cerebellar Circuit

The cerebellum is composed of tightly folded layers of gray matter – the cerebellar cortex – with white matter beneath composed of myelinated fibers projecting to and from the cerebral

cortex (Eccles et al., 1967). Within the white matter, there are three pairs of DCN: fastigial, interpositus and dentate.

The cerebellum has a highly regular structure and is composed of repeating neuronal units each with the same basic microcircuitry. The cerebellar cortex contains three layers composed of distinctive types of neurons. The deepest one is the granule cell layer and receives inputs to the cerebellum. It is densely packed with granule cells (GCs), the most abundant cell type in the brain, as well as interneurons, such as Golgi cells. Part of this layer is occupied by cerebellar glomeruli, a structure composed of excitatory synapses between mossy fibers (MFs), GCs and Golgi cells. In the Purkinje cell layer lies the cell bodies of PCs, whose axons are responsible for the sole output of the cerebellar cortex forming GABAergic synapses with the DCN. DCN neurons subsequently make excitatory synapses with their targets, such as brainstem nuclei and the cerebral cortex. Lastly, the molecular layer is the most superficial one and is built up of GC's axons referred to as parallel fibers (PFs) because of their longitudinal display. Additionally, this layer is also composed of inhibitory interneurons (molecular layer interneurons; MLIs) as well as the extension of PC's dendrites, where both parallel and climbing fibers (CFs), another main input source of the cerebellum, synapse (Eccles et al., 1967).

Mossy Fibers – Granule Cells

Each GC receives an average of four inputs from MFs that originate from cell bodies in the spinal cord and brainstem, receiving sensorial context information from both the cerebral cortex and the periphery (Eccles et al., 1967). Multimodal pathways converge onto individual GCs, making a highly diverse stream of information being conveyed to the cerebellar cortex (Huang et al., 2013). PFs synapse with three hundred PCs on average but each produces brief, small excitatory effects on PCs, thus requiring a summation of a large number of PFs' action potentials to generate rapid, high-rate depolarizations – referred to as simple spikes (Eccles et al., 1967; Martinez et al., 1971; Chadderton et al., 2004).

Climbing Fibers

CFs are one of the main sources of input to the cerebellum. They originate from a specific nucleus of the brainstem, the inferior olive, and carry information from all sensorial systems (consisting mainly of sensorial feedback). Each CF forms excitatory synapses with up to ten

PCs, establishing several points of contact with PCs in a 1:1 ratio (Rescorla, 1988). Although only one CF synapses with PCs, its influence upon PC's activity is markedly different from PFs, producing complex spikes as a result of prolonged depolarization. CFs, like PFs, also spontaneously generate action potentials, but with low spike rates instead (Eccles et al., 1967; Martinez et al., 1971).

Molecular Layer Interneurons

MLIs, traditionally known as basket and stellate cells, are inhibitory interneurons that receive direct excitatory inputs from GCs (Eccles et al., 1967; Mittmann et al., 2005). These cells have spontaneous activity and strongly inhibit PCs and other MLIs, modulating PC output (Kim, Augustine, 2021).

1.2.2.2 Eyeblink Conditioning Circuit

The neuronal circuit underlying eyeblink conditioning is relatively well-established (Figure 1.2), with CFs conveying the error signals (air puff US) (Mauk et al., 1986; Steinmetz et al., 1989; Welsh, 1998), and MFs the information about the sensorial context (light CS) (Steinmetz et al., 1988; Hesslow et al., 1999). Additionally, GCs have been the center of cerebellar learning theories for decades (Marr, 1969; Albus, 1971; Ito, 1972), and recently, have been found to be key components in eyeblink conditioning adaptive responses (Giovannucci et al., 2017).

1.2.3 Synaptic Plasticity

As aforementioned, the ability of the cerebellum to produce accurately timed CRs occurs in a time-dependent manner, through repeated pairing of the CS with the US, causing synaptic changes (De Zeeuw, Yeo, 2005). According to the Marr-Albus-Ito theory, when PF-PC and CF-PC synapses are reliably active at the same time, modifications occur at the PF level (Marr, 1969; Albus, 1971; Ito, 1972). This hypothesis was corroborated by Ito's results that showed that the combined activation of these pathways resulted in long-term depression (LTD) of the PF-PC synapse. LTD in PF-PC synapse by CF input improves learning by decreasing the strength of error-associated PF-PC synapses, leading to changes in PC's output (Carey, 2011).

Nonetheless, recent work has highlighted that PF-PC LTD cannot account for every aspect of cerebellar dependent learning and that there are several types and sites of plasticity that

may have different roles in motor learning and memory (De Zeeuw, Yeo, 2005; Carey, 2011; Antonietti et al., 2017). Besides synaptic plasticity at the PF-PC level, interneurons' (such as MLIs) modulatory role in timing and regularity of PC's spiking may also be implicated in motor performance (Boele et al., 2018; Kim, Augustine, 2021). Studies have also shown the involvement of synaptic plasticity of the DCN in learning of eyeblink conditioning (Carey, 2011), especially at the level of MF-AIP synapse (Ohyama, Mauk, 2001; Pugh, Raman, 2006; Zhang, Linden, 2006; Freeman, Steinmetz, 2011). Finally, AIP learning seems to depend on the association of both excitatory and inhibitory inputs coming via MF and PC, respectively (Pugh, Raman, 2006).

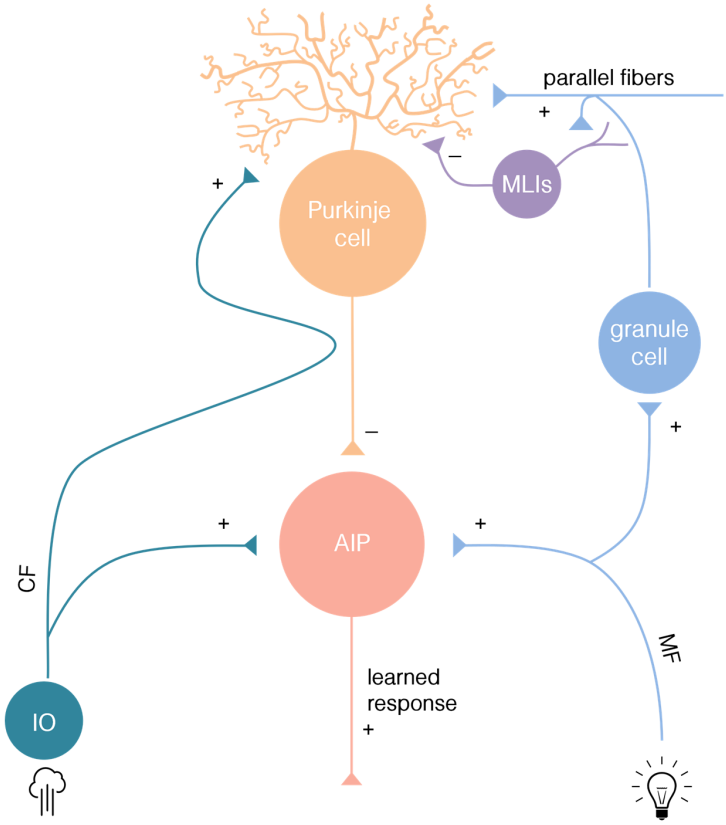

Figure 1.2: Diagram of the cerebellar circuit underlying eyeblink conditioning. During eyeblink conditioning, climbing fibers (CF) relay the information about the learning instruction (air puff US), while mossy fibers (MF) relay information regarding the learning context (light CS). Granule cells also form excitatory synapses with molecular layer interneurons (MLIs), which inhibit Purkinje cells and modulate their output. This information is integrated into the cerebellar cortex, from where Purkinje cells transmit the output to the anterior interpositus nucleus (AIP), which then regulates motor behavior. Adapted from Kandel (2013).

1.2.4 Modulation of Learning by Locomotion

It is clear that the cerebellum regulates motor coordination and locomotion. Notwithstanding, locomotion has also been shown to modulate the cerebellar cortex's activity, mainly through increased MFs and consequently GC's activity (Ozden et al., 2012; Powell et al., 2015; Muzzu et al., 2018).

Interestingly, it has been recently demonstrated that locomotion positively modulates the acquisition and expression of eyeblink conditioning (Albergaria et al., 2018). Mice that run more while performing the eyeblink conditioning task learned faster. Runners not only developed CRs earlier but also had trial-by-trial enhancement of the responses, in a speed-dependent manner. When running on a motorized treadmill at a constant speed, inter-animal variability was also greatly reduced. As multimodal input from MFs induces suprathreshold firing activity at GCs (Ishikawa et al., 2015), MF increased activity during locomotion (Powell et al., 2015) combined with CS signals (visual, auditory or tactile) may allow GCs to more efficiently compute eyeblink associated information (Albergaria et al., 2018).

1.3 Cerebellar Motor Memory Consolidation

1.3.1 Memory Consolidation

Memory consolidation can be defined as a set of processes whereby a labile memory progressively becomes more stable. Memory is considered stabilized when it becomes resistant to interference, such as the formation of a competing memory or a localized lesion (Dudai, 2004).

Consolidation is commonly viewed in two types: synaptic consolidation and systems consolidation (Dudai, 2004; Dudai et al., 2015). The first one involves modifications at the cellular level that stabilize synaptic plasticity after learning, occurring within minutes to hours after the encoding (Dudai, 2004; Kandel et al., 2014). Whereas systems consolidation consists of the gradual reorganization of memory representations over distributed brain areas, taking longer to be established (weeks, months or years) (Dudai, 2004). While the foundational aspects of synaptic consolidation are considered universal, systems consolidation has been investigated mainly in declarative memories. Thus, it is usually described as the process by which memories get reorganized into the neocortex, eventually becoming independent from the

hippocampus (Squire, Alvarez, 1995; Dudai, 2004; Dudai et al., 2015; Squire et al., 2015). Interestingly, the local molecular and synaptic alterations may occur simultaneously to the circuitry rearrangement and, by working together, they make consolidation a continuous process (Dudai, 2012).

Moreover, declarative and procedural knowledge have different natures; while declarative memory involves the conscious recall of information comprising the medial temporal lobe and hippocampus, procedural memory does not require awareness and usually involves the motor cortex, striatum and cerebellum (Squire, Dede, 2015).

1.3.2 Consolidation of Eyeblink Conditioning Responses

Retention of eyeblink learned responses also requires the cerebellum: post-training reversible inactivation of the eyelid region of the cerebellar cortex using the GABAA receptor agonist muscimol disrupted consolidation of learned responses (Attwell et al., 2002). It was observed that infusions of muscimol five minutes after the end of the learning sessions were able to prevent consolidation (Attwell et al., 2002), and it was established that the infusion should be done between five and forty-five minutes after the sessions for greater impairment (Cooke et al., 2004). These results suggest that the cerebellar cortex is crucial for the consolidation of cerebellum-dependent motor memories in rabbits. However, eventually, the dependence on this structure appears to be reduced since infusions ninety minutes post-training had little or no effect. Moreover, Cooke et al. (2004) identified a 2-hour time window for consolidation to occur, starting around 1 hour after training, and suggested parallel fiber LTD as the main probable mechanism for this process.

On the other hand, reversible inactivation of the eyeblink conditioning nuclei region (AIP) after the sessions of learning, similar to the one performed in the cerebellar cortex, had null effects on consolidation (Attwell et al., 2002). This result has also been reinforced by other studies, suggesting that the consolidation process of cerebellum-dependent motor memories mostly resorts on the cerebellar cortex and not on the DCN/AIP, at least in earlier stages (Kellett et al., 2010). However, it has been hypothesized that these types of memories also present circuitry reorganization involving the DCN/AIP - systems consolidation (Kassardjian et al., 2005; Shutoh et al., 2006). Similar to declarative memory, cerebellum-dependent memory traces would be encoded initially in the cerebellar cortex as a result of rapid plasticity and then, after gradual changes in PC firing and synaptic plasticity, shift its anatomical location to the

DCN/AIP (Medina et al., 2001; Ohyama, Mauk, 2001).

Granule cells have also been implicated not only in the acquisition phase (Giovannucci et al., 2017) but also in memory consolidation of cerebellar adaptive responses (Galliano et al., 2013). Disruption of long-term plasticity between PFs and PCs proved to impair learning and consolidation of learned responses of cerebellar-dependent tasks (Galliano et al., 2013). However, the role of these cells in the consolidation of eyeblink conditioning learned responses has yet to be investigated.

Interestingly, MLIs have also been suggested to have a relevant role in the consolidation of cerebellar-dependent memories. These cells are also a site for plasticity and their feedforward inhibition of PCs appears to have an important modulatory effect on them, regulating memory consolidation (Wulff et al., 2009).

Overall, these findings suggest that cerebellar motor memories are consolidated and stored, at least initially, in the cerebellar cortex, and that GCs potentially have a primary role in this process. How the DCN/AIP are involved in the consolidation of cerebellar motor memories, specifically on eyeblink conditioning in mice, has yet to be established. Are cerebellum-dependent memories consolidated similarly to other systems? Do eyeblink learned responses also show synaptic and system consolidation properties?

1.4 Aims

Our main goal was to investigate the dynamics of motor memory consolidation of mice in a cerebellar-dependent learning task, eyeblink conditioning. We performed reversible inactivations of the cerebellar cortex post eyeblink conditioning training sessions, f ollowing up on data previously acquired in the laboratory (Silva et al., in preparation). To precisely target the consolidation time period of eyeblink learned responses, we took advantage of optogenetic tools to specifically target GCs, a main component of the cerebellar cortex. This allowed us to study the temporal properties of consolidation as well as evaluating the importance of GCs for this process. Further, to assess a possible shift in eyeblink conditioning memory storage, we have performed reversible inactivations i) of the cerebellar cortex at later more stable stages of learning, and ii) of the AIP after each acquisition session to investigate whether this structure was being recruited at an earlier stage of learning.

Chapter 2

Materials and Methods

2.1 Animals

All procedures were performed in different mouse lines with C57BL/6J background. Both males and females mice were used. Mice used were between 10 and 14 weeks of age and had not been used in any prior experiments.

Mice were housed in standard cages in groups of 2 to 5 with food and water *ad libitum*. Very sporadically animals had to be single-housed, especially males, due to disruption of normal behavior, such as display of aggression and barbering (over-grooming or fur plucking). Mice were kept on a reverse light cycle (12 hr light/12 hr dark) so that experiments were conducted during the period mice were more active.

All procedures were carried out in accordance with the European Union directive 86/609/EEC and approved by the Portuguese National Authority for Animal Health (Direção Geral de Alimentação e Veterinária – DGAV).

2.1.1 Mouse Lines

For the reversible inactivation experiments, we used WT from C57BL/6J or, when unavailable, littermate controls of the other mouse lines available in the laboratory.

For the optogenetic experiments we used mouse lines that express either channelrhodopsin-2 (ChR2) or archaerhodopsin-3 (ArchT) specifically on granule cells (GC); Gabra6cre-ChR2-YFP (GC-ChR2) and Gabra6cre-ArchT-GFP (GC-ArchT), respectively. These mouse lines were obtained by crossing Gabra6-Cre mice, in which Cre recombinase expression was driven

by the alpha6 subunit of the GABAA receptor (Fünfschilling, Reichardt, 2002), with either ChR2-EYFP-LoxP or ArchT-GFP-LoxP from the Jackson Laboratory (stock number 012569 and 012735, respectively). As controls for each experiment, we used the WT littermates for each condition.

2.1.2 Surgical Procedures

In all surgeries, animals were anesthetized with isoflurane *(IsoFlo - Zoetis)* - 4% induction and 0.5-1.5% for maintenance - and placed in a stereotaxic apparatus *(David Kopf Instruments, Tujunga, CA)*. In the beginning, both eyes were covered with a gel *(Vidisic gel, Bausch Lomb)* to prevent eye drying. Mice were then intraperitoneally injected with a non-steroidal anti-inflammatory and analgesic *(Carprofen, in-house vivarium made)*. The head was cleaned with ethanol and povidone-iodine before a 1 cm diameter circle of skin was cut to expose the skull. A craniotomy was drilled over the eyelid area of the cerebellar cortex (AP -5.7, ML +1.9) or over the AIP cerebellar nucleus (AP -6, ML -1.7) after the appropriate brain alignment.

For the reversible inactivation experiment, a 26 gauge, 5 mm length guide cannula *(PlasticsOne)* was implanted at the surface of the brain. In order to target the infusion to the eyelid area of the cerebellar cortex (lobule IV/V; Chettih et al., 2011), an internal cannula projecting 1.5 mm was later inserted into this guide cannula during experiments. To target the cerebellar nucleus (AIP; Chettih et al. (2011)), the guide cannula was implanted 0.2 mm below the surface, and an internal projecting 1.8 mm was then used.

For the optogenetic perturbation, a 100 µm diameter, 3 mm length, 0.22 NA optical fiber *(Doric Lenses)* was implanted, at the eyelid area of the cerebellar cortex (AP -5.7, ML +1.9, DV -1.5). Additionally, a metal head piece (headpost) was transversally attached to the surface of the skull over *bregma*. Both the implant (infusion cannula or optical fiber) and the headpost were fixed into place using dental cement *(Super Bond, CB)*.

2.2 Conditions

2.2.1 Setup

The experimental setup was based on previous work in the laboratory (Albergaria et al., 2018) (Figure 2.1 A). Head-fixed mice were placed on top of a running apparatus consisting

of a fast-trac activity wheel mounted on top of a mouse igloo *(Bio-Serv)*. Depending on the experiment, the running wheel was either freely rotating by mouse impulse (self-paced) or externally maintained at a fixed speed (motorized; usually 0.10 m/s for medium speed). The speed of the motorized running wheel was controlled by a DC motor with an encoder *(Maxon)*. Running speed was measured using an infrared sensor placed underneath the running wheel *(PTRobotics)*. The setup was placed inside a soundproof box kept in the dark and mice were monitored using a surveillance camera *(PlayStation Eye)*.

2.2.2 Stimuli

The stimuli used were in accordance with the standard procedure done in the laboratory (Albergaria et al., 2018) (Figure 2.1 B). The unconditioned stimulus (US) had to reliably elicit a full blink, so we delivered a puff of air (40 psi, 50 ms duration) controlled by a Picospritzer *(Parker)* through a needle positioned in front of the right eye. The conditioned stimulus (light CS) had to be neutral but salient enough to be detectable by both eyes, thus, as the mouse is placed inside a dark box, we used a white LED (350 ms duration) positioned 2-3 cm directly in front of it.

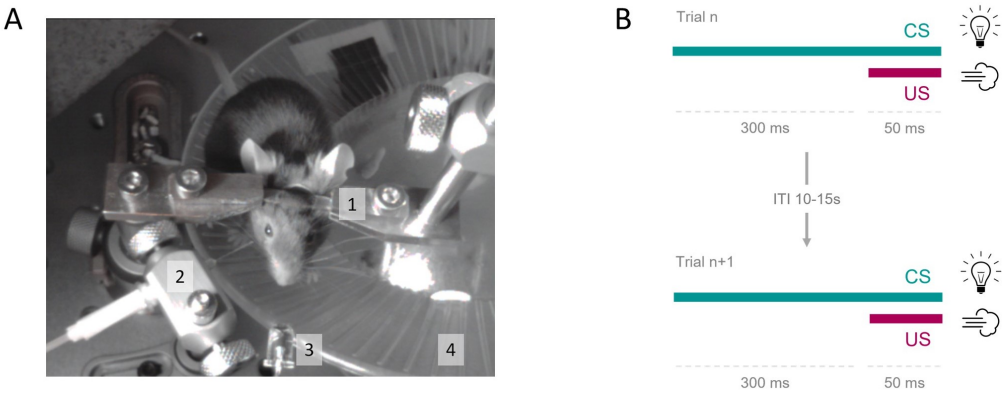

Figure 2.1: Delay eyeblink conditioning experimental setup with head-fixed apparatus and protocol. A) Experimental setup - 1) head-fixed mouse, 2) air puff needle for air puff US delivery, 3) LED for light CS presentation, 4) treadmill with a sensor coupled for running measurement assessment. **B)** Eyeblink conditioning trial structure - Each acquisition session of eyeblink conditioning had an average of 100 or 40 trials, for long and short session protocols. The light CS had a 350 ms duration while the air puff US had a 50 ms. The stimuli were separated by a 300 ms fixed interval and co-terminated. Each trial was separated by a randomized intertrial interval (ITI) of 10 to 15s.

2.2.3 Reversible Inactivation

For the reversible inactivation, we used muscimol *(Sigma-Aldrich)*, a GABAA receptor agonist diluted at a 1 mM concentration into a brain-buffer vehicle solution (ACSF, Artificial

CerebroSpinal Fluid; *RD Systems*). By the end of each session, either muscimol or vehicle were delivered through an internal cannula that went 1.5 mm or 1.8 mm down the guide cannula, to target the eyelid area of the cerebellar cortex or the AIP cerebellar nucleus, correspondingly. These substances were infused for 5 min at a 100 nL/min rate, making a total of 500 nL. After infusion, a dummy cannula *(PlasticsOne)* was placed on the guide cannula to keep it clean and unclogged, and to protect the brain from possible infections. To further reduce contamination, the internal cannula was disinfected with 70% ethanol in between animals.

2.2.4 Optogenetic Perturbation

For the optogenetic experiments, lights from either 473 nm (blue) or 595 nm (yellow) lasers *(Laserglow Technologies)* were used to perturb or inhibit cellular activity, accordingly. Laser lights were delivered through an optogenetics patch cord (100 μm core diameter, 0.22 NA) that connected to the optical fiber implanted in the animal's brain (zirconia tip, sleeve connection). The animals expressed either blue (GC-ChR2) or yellow (GC-ArchT) light-driven rhodopsins specifically on granule cells. ChR2 is a cation channel activated in response to blue light, depolarizing the cells, while ArchT is a proton pump activated in response to yellow light, hyperpolarizing and inhibiting the cells (Bernstein, Boyden, 2011).

2.2.5 Data Acquisition

Videos of the eyelid movements were recorded using Genie HM640 *(DALSA)* monochromatic camera to monitor a 172 x 160-pixel region, so it enclosed the whole eye, at 900 fps. The recordings were performed so that each trial had a corresponding video. Lighting was provided by an infrared light *(Infaimon)*.

A custom-written code in LabVIEW together with a board responsible for digital to analog signal conversion (both from *National Instruments*) were used to trigger and control all the hardware in a synchronized way.

2.3 Protocol

After the surgical procedures and handling, mice were habituated to the setup for at least 3 days prior to training (4 sessions for the motorized running wheel and 6 sessions for the self-

paced running wheel). During habituations mice were placed on top of the running wheel for gradually increasing durations from 5 to 20 minutes without stimuli being presented.

For each session, mice were head-fixed while under light isoflurane anesthesia to decrease the animals' stress (mice would wake up within 10 to 15 s while we adjusted the setup conditions). Most experiments consisted of three phases: acquisition, test and extinction. During acquisition, mice were presented with 90% CS-US paired trials and 10% CS-only trials in a pseudo-randomized order (in each block of 10 trials, 9 were CS-US and 1 was CS-only). CS-only trials allowed us to observe the full dynamics of the learned responses, since they are not masked by the unconditioned response (UR) to the airpuff US. Mice performed one session a day and each session had on average either 100 or 40 trials (for long or short sessions). Trials were separated by a randomized intertrial interval (ITI) of 10 to 15 s. The onsets for the light CS and air puff US were separated by a fixed interval (ISI - InterStimulus Interval) of 300 ms, and both stimuli co-terminated in time (Figure 2.1 B). The test phase was different depending on the experiment; detailed below. By the end, animals performed 4 extinction sessions which consisted of 100% of CS-only trials.

2.3.1 Reversible Inactivation

As mentioned, for the reversible inactivation experiments, we performed infusions in WT animals. The acquisition phase on the self-paced running wheel consisted of 14 sessions (S1-S14) while on the motorized it had a 10-session duration (S1-S10).

Mice were randomly assigned either to muscimol or vehicle-treated group. 5 minutes after each learning session, mice were infused with either muscimol or vehicle while remaining head-fixed on the running wheel (Figure 2.2). Each infusion lasted 5 min so that by the end 500 nL of either substance was injected. After the infusion was complete, mice stayed head-fixed on the running wheel for an additional 5 min to properly deliver the solution. After 6 hours, muscimol's effect decreases (Cooke et al., 2004), therefore mice's performance was only re-assessed 24 hours later when muscimol had already been washed out of the mouse's organism.

The test phase of these experiments was done to evaluate if the muscimol infusions had been performed in the appropriate eyeblink location. Thus, after the last acquisition session, all mice received a muscimol infusion (equal to the ones performed during acquisition), and their learning was assessed 5 to 10 min after in a short 30-trial session (muscimol test; M1). If the cannula was well-placed the animals would not be able to exhibit previously acquired conditioned

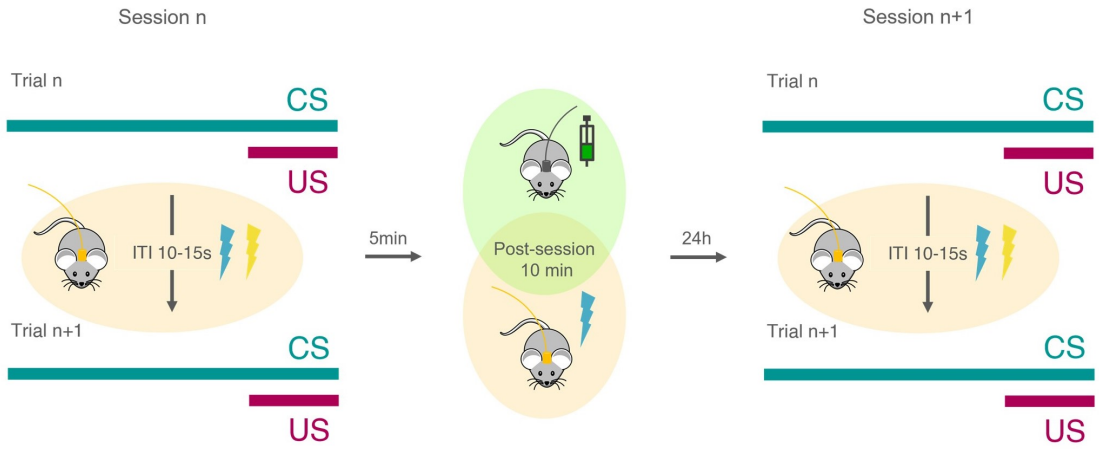

Figure 2.2: Protocol for within and post-session perturbations. We have performed two types of perturbations of the cerebellar cortex: within the learning session and post-session. To specifically target the intertrial interval (ITI) of each learning session, we used optogenetic tools to perturb granule cells during this period. We used GC-ChR2 and GC-ArchT mice, which got either 473 nm or 595 nm laser lights, depicted as blue or yellow lightening bolts, respectively. During every learning session, 5 ms pulses of light were delivered at 100 Hz during the ITIs for 5 s to perturb or inhibit granule cell's activity. The ITI had a 10 to 15 seconds duration and laser stimulation randomly occurred for 5 s during this period. The same procedure occurred in every ITI of the 15 sessions of acquisition. On the other hand, to perturb the post-session period, we performed either reversible inactivation using muscimol or optogenetic perturbation. 5 min after every learning session, mice would either be infused with 500 nL of muscimol or vehicle (green syringe), or optogenetically perturbed (blue lightening bolt) for 10 min while remaining on the running wheel. The optogenetic perturbation consisted of interspersed laser stimulation delivered at 100 Hz for 5 s every 10-15 s, randomized. For both types of perturbations, mice's learning was reassessed the next day and the same procedure was repeated for the rest of the acquisition phase.

responses (as described in Attwell et al. (2002); Cooke et al. (2004)). Additionally, in some experiments, to account for the effect of the procedure itself, on the following day all mice were tested with a 30-trial session after a vehicle infusion instead (vehicle test; V1). Additionally, to properly confirm the placement of the cannula for the reversible inactivation experiments on the AIP, we performed histological microscopy. As infusions to both the cerebellar cortex and the AIP prevent the expression of previously acquired learned responses (Attwell et al., 2002; Heiney et al., 2014), we needed to ensure that the infusions were specifically targeting the AIP, and not the cerebellar cortex (Figure 2.3 A, B). After the test phase, mice underwent 4 sessions of extinction (E1-E4).

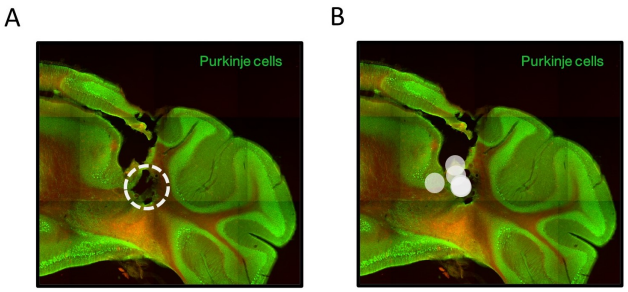

Figure 2.3: Validation of infusion cannula placement at the AIP cerebellar nucleus. A) Histological sample for a representative animal indicating cannula placement at the AIP. Dashed white circle indicated cannula track. **B)** Histological samples with gray circles indicating guide cannula placement above the AIP, for each animal.

2.3.1.1 Control experiment for running during infusion

To assess the importance of running during the infusion protocol, mice performed the acquisition sessions on the self-paced running wheel and were immediately transferred to the motorized running wheel for the infusion protocol. As for the main protocol, the infusion lasted 5 min and the animals stayed for an additional 5 min. The process of transferring the animals from the self-paced to the motorized running wheel and the start of the infusion took, on average, 5 min as well.

2.3.1.2 Control experiment for infusion after the acquisition phase

A subset of the reversible inactivation animals learning on the self-paced running wheel underwent an experiment done to evaluate the effects of muscimol after the animals had already learned (after acquisition; P1-P4). Similar to the acquisition phase, mice were infused with muscimol at the end of the session, and their learning was re-assessed on the following day. This experiment was performed in mice that had had vehicle infusions during acquisition so that they had minimal contact with muscimol before (only infused for the test session, M1).

2.3.2 Optogenetic Perturbation

As mentioned, for the optogenetic experiments, we used GC-ChR2 or GC-ArchT mice. These animals did 15 sessions of acquisition (S1-S15) independent of being on the motorized or on the self-paced running wheel. The optogenetic perturbation was done either during or after the learning session depending on the experiment, as detailed below (Figure 2.2). After the acquisition sessions, we performed a test consisting of interleaved blocks of 10 trials each (test blocks) where blocks without laser were followed by blocks with laser-driven perturbation in between trials. There were a total of 10 blocks (T1-T10) for the long and 6 blocks (T1-T6) for the short sessions. With this, we assessed whether laser perturbation in between the trials was affecting the cells' ability to respond on the next trial. After the test blocks, mice underwent the extinction protocol (E1-E4).

We verified the proper location of the optogenetic fiber placement at the eyelid region of the cerebellar cortex of GC-ChR2 mice by measuring the eyeblink response to specific laser power stimulations (test blink; Figure 2.4 A). GC-ChR2 mice present a blink to the laser because GCs' stimulation activates MLIs which in turn strongly inhibit PCs, causing a pause

in their activity. This pause in PC activity causes disinhibition of the DCN and consequentially an eyeblink. The laser power used during the experiments was adjusted to detect a subtle eye movement (stimulation almost subthreshold), causing only a mild perturbation of GCs baseline neuronal activity. Corresponding laser powers were chosen for GC-ChR2 animals and their littermates, and overall, they were similar among all optogenetic experiments (Figure 2.4 B). Laser power ranged from 1 to 3 mW, with an average of 2.9 mW (63.64 of irradiance, https://web.stanford.edu/group/dlab/optogenetics) for the blue light. The test blink was performed both at the beginning (to select animals) and at the end of the experiment (to confirm the functionality of laser stimulation).

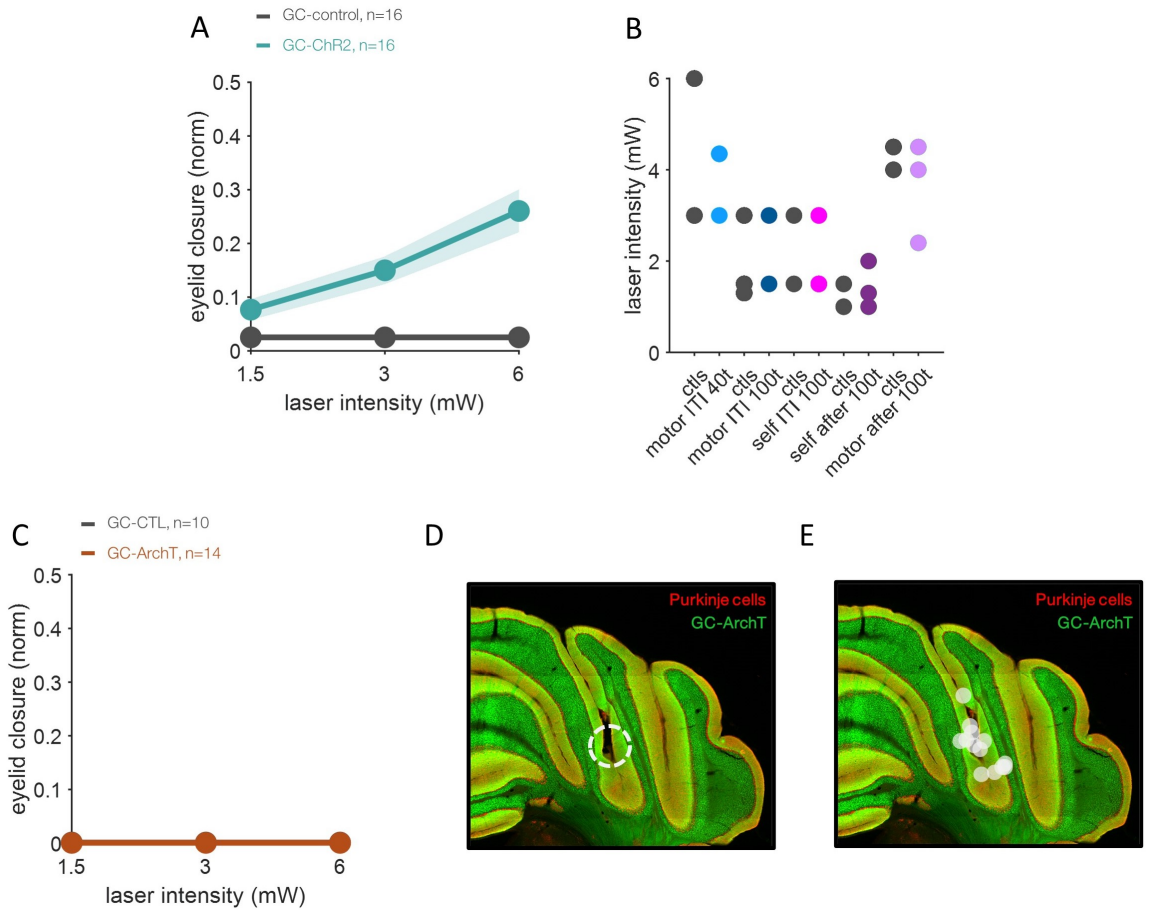

Figure 2.4: Validation of optic fiber placement at the eyelid area of the cerebellar cortex for GC-ChR2 and GC-ArchT. To validate the fiber placement for GC-ChR2 mice, we measured their eyeblink movements in response to specific laser powers, while for GC-ArchT we need to find the optic fiber track through histology. **A)** Range of laser power used on GC-ChR2 experiments: optogenetic perturbation of the ITI on the motorized (40t, blue; 100t, dark blue) and on the self-paced running wheels (pink); and post-session optogenetic perturbation on the self-paced (purple) and on the motorized running wheels (lilac). GC-CTLs are represented in gray. **B)** Amplitude of laser-driven eyeblink for 1.5, 3 and 6 mW for GC-ChR2 mice. Shaded error bar represents standard error of the mean (SEM). **C)** Amplitude of laser-driven eyeblink closure for GC-ArchT mice. **D)** Histological sample for a representative animal indicating fiber placement at the eyelid region of the cerebellar cortex. Dashed white circle indicates fiber track. **E)** Histological sample indicating fiber placement for all GC-ArchT animals. Fiber track depicted as superimposed gray circles. Green fluorescence indicates ArchT-GFP expression and red Purkinje cells.

On the other hand, as GCs' inhibition is not strong enough to inhibit PCs' tonic firing, GC-

ArchT mice do not present a laser-driven blink (Figure 2.4 C). Thus, we had to confirm their fiber placement by locating the fiber track in histological slices (Figure 2.4 D, E). The laser power was set at 6 mW (190,91 of irradiance) to increase the likelihood of cells being affected.

The laser power was adjusted for each animal and measured with a power meter *(Thorlabs)* at the beginning and at the end of every session.

2.3.2.1 Optogenetic perturbation during the session (ITI)

To test the hypothesis of consolidation occurring within the learning sessions, 5 ms pulses were delivered at 100 Hz for 5 s in between the trials (ITI; 10-15s) of the acquisition sessions (Figure 2.2). This experiment was done in both GC-ChR2 and GC-ArchT on the motorized and self-paced running wheel. In some experiments, we also included catch trials (10%) where no stimulation was delivered in between the trials to be able to measure its impact on the expression of learning on the next trial.

2.3.2.2 Post-session optogenetic perturbation

As a complementary experiment to understand the effects of laser stimulation after each learning session and to compare to the muscimol post-session infusions, we optogenetically perturbed the post-session period (Figure 2.2). For this experiment, we used GC-ChR2 mice learning on either the self-paced and motorized running wheel. This protocol started 5 min after the end of each session and consisted of a 10 min interspersed laser stimulation (5 s 100 Hz stimulation every 10-15 s).

2.4 Histology

Animals were perfused transcardially with 4% paraformaldehyde and their brains were removed so that fiber or cannula placement could be examined. Coronal sections were cut on a vibratome and mounted on glass slides with Mowiol mounting medium. Histology images were acquired with an upright confocal laser point-scanning microscope *(Zeiss LSM 710)*, using a 5× or 10× objective. Brain slices were stained for calbindin (Purkinje cells) and DAPI (nucleus). GC-ChR2 and GC-ArchT mice expressed a fluorescence tag. To evaluate the target and spread of muscimol infusions, fluorescent muscimol was infused prior to perfusion.

2.5 Data Analysis

Data analysis was performed using Matlab *(Mathworks)* software. Recorded videos were analyzed post-hoc using a custom-written code, previously developed in the lab.

2.5.1 Behavioral Analysis

For each video recording, eye closure was measured by the distance between the eyelids. This was calculated frame by frame by thresholding the grayscale image of the eye's outline and extracting the count of pixels that constituted the minor axis of the elliptical eye-region (Figure 2.5 A). Eyelid closure was normalized for each session of each mouse so that the pixel size was 0 for the eye fully open and 1 for a full blink. The eyelid position in the 0.1 s preceding each trial was subtracted from that trial, resulting in all of the trials starting from 0 (eye open). An eyelid movement was considered a CR if a) it occurred between 0.1 s after the light onset and the beginning of the airpuff delivery and b) it exceeded 10% of full eye closure ($>$ 0.1 normalized pixel values).

Average traces of the eyelid responses as mean values of all trials per time point were calculated for each session (Figure 2.5 B). Average CR amplitudes were calculated for each session as the mean value of eyelid closure of the CRs and plotted as a function of time (number of sessions).

2.5.2 Statistical Analysis

Statistical analysis was performed using the Statistics toolbox in Matlab software, in a custom-written code. To quantify the statistical difference of both CR percentage and amplitude during learning acquisition in each experimental condition (experimental vs littermate controls), we used a 2-sample independent t-test. Because the levels of learning of control animals are different across the several experiments we have performed (self-paced vs motorized, WT vs transgenic mice, etc), we used the maximum learning acquired in each control group to normalize learning across conditions. The first session of learning used for statistical comparison was selected from the littermate control learning average curve as the first to surpass the normalized threshold of 30% for the %CR or the 0.3 for the CR amplitude; statistical analysis was performed from that session onwards, in both control and experimental groups. To quantify

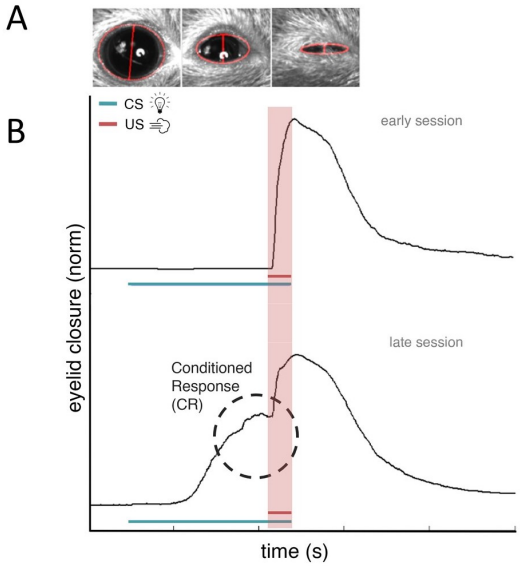

Figure 2.5: Analysis of eyeblink conditioning trials throughout learning. **A)** Eyelid movements recorded for each trial - To analyze the eyeblink kinematics, the distance between the eyelids was measured in pixels for each trial. **B)** Average traces of a learning session of delay eyeblink conditioning - In early sessions the mouse only blinks to the air puff US, whereas, after the presentation of several hundred paired trials, the animal learns to close the eye in response to the light CS before the air puff US onset - which is called a conditioned response (CR).

the statistical difference of both CR percentage and amplitude during the extinction phase, we did a 2-sample independent t-test to compare the mean value for each animal in each condition of the 4 sessions of extinction. The statistical measurement of the difference of CS-only trials between the groups was done by a 2-sample independent t-test, comparing the maximum eyelid closure of each animal in each condition by the end of learning in the experimental vs littermate controls. The statistical analysis for the test blocks and catch trials was done through the comparison of the maximum eyelid closure for each animal in each condition (CTL or GC-ChR2/GC-ArchT; baseline or laser) between 0.1 and 0.3 s after the CS onset (identical to the time interval for considering an eye movement a CR). This was done by a 2-sample paired t-test, comparing the data from the control group in the presence of laser (CTL laser) and without it (CTL baseline), and the experimental group with the presence of the laser (ChR2/ArchT laser) and without it (ChR2/ArchT baseline). Differences were considered statistically significant when the p-value was *$p<0.05$, **$p<0.01$, ***$p<0.001$.

Chapter 3

Results

To investigate motor memory consolidation, we assessed the learning of mice in an eyeblink conditioning task (Silva et al., in preparation). These experiments were performed as described previously, with head-fixed mice walking on a running wheel (Albergaria et al., 2018). We evaluated the ability of mice to learn to close their eyes in response to a LED (light CS) after consistently pairing it with an air puff (air puff US). As a measure of learning, we calculated the percentage of learned responses to the light CS before the air puff US was presented - %CR.

3.1 Reversible inactivation of the cerebellar cortex

3.1.1 Post-session muscimol infusions interfere with the memory consolidation of animals learning while walking on a self-paced running wheel

To study the role of the cerebellar cortex in the consolidation of eyeblink conditioning learned responses in mice, we performed reversible inactivations of the cerebellar cortex immediately after each session of learning, similarly to previous studies done in rabbits (Attwell et al., 2002; Cooke et al., 2004) (Figure 3.1 A-C). For that, we infused muscimol, a GABAA receptor agonist, which affects the cerebellar cortex's activity. We trained two randomly assigned groups of mice on eyeblink conditioning to either receive post-session muscimol (N=11) or vehicle (N=4) infusions, while they were on the self-paced running wheel.

Consistent with the literature (Attwell et al., 2002; Cooke et al., 2004), mice infused with

muscimol right after each session of learning had delayed acquisition of eyeblink responses when delayed in acquisition, they eventually reached levels of learning comparable to their littermate controls (Figure 3.1 D, F). Mice infused with muscimol also presented a decrease in CR amplitude, when compared to the control group (Figure 3.1 E).

To confirm if the infusions were being delivered specifically to the eyelid region of the cerebellar cortex, we performed a test at the end of the acquisition phase where we injected muscimol before instead of after it (M1; Figure 3.1 D shaded green bar) (Attwell et al., 2002; Cooke et al., 2004). We observed a decrease in CRs upon muscimol injection, which confirms the cannula placement. This also indicates that cells in this area were still sensitive to muscimol treatment by the end of the acquisition phase. We applied this procedure to both muscimol and vehicle-treated animals, and mice that did not decrease in M1 were excluded. No differences between the two groups were observed neither in M1 nor in the extinction phase (Figure 3.1 D, E).

Similar to the experiments done in Attwell et al. (2002), we performed muscimol post-session infusions in mice that had completed the acquisition phase as vehicle controls. This was performed to evaluate the effects of cerebellar cortical inactivations in already acquired memories. Our results indicate that cerebellar cortex inactivation after mice have already acquired eyeblink conditioning responses does not affect their consolidation (Figure 3.1 G), in accordance with previous literature (Attwell et al., 2002).

These results indicate that the cerebellar cortex is necessary for the consolidation of eyeblink responses in mice. Additionally, similar to previous results in the laboratory (Albergaria et al., 2018), mice running at a faster speed appeared to be less susceptible to the muscimol effect. This raised the question of whether the memory consolidation process can be modulated by running.

3.1.2 Running makes memory consolidation less susceptible to post-session muscimol infusions

Data from the laboratory has shown that animals running faster on the self-paced learned faster as well, however, self-paced running is variable and usually restricted to slow speeds (Albergaria et al., 2018). Therefore, to appropriately evaluate the effects of running on motor memory consolidation, we externally controlled the speed at which animals walked during the

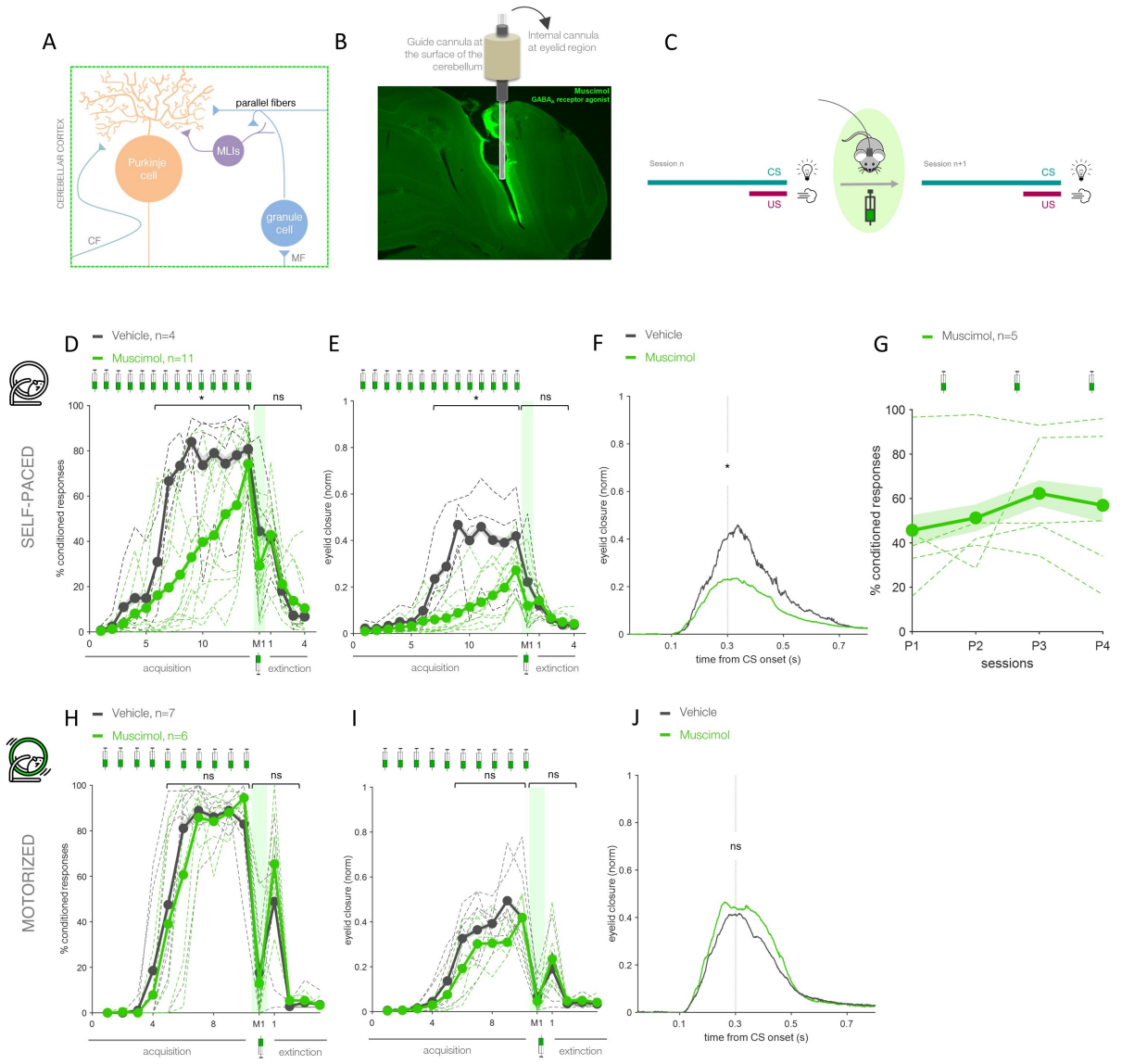

Figure 3.1: Running modulates the effect of post-session reversible inactivations of the cerebellar cortex on the consolidation of eyeblink learned responses. To study the effect of running on consolidation of eyeblink learned responses, we performed post-session reversible inactivation of the cerebellar cortex in two running contexts: voluntary walk on the self-paced running wheel or active walk on the motorized running wheel. **A)** Cerebellar circuit diagram representing the cerebellar cortex (dashed green square) as the target area for muscimol infusions. **B)** Representative fluorescence image of a coronal cerebellar slice showing the cannula track in the eyelid sulcus of the cerebellar cortex. Depicted in the figure is also the guide cannula implanted at the surface of the cerebellum through which the internal cannula is introduced to acutely deliver the infusions to the eyelid area. **C)** Schematics of post-session muscimol infusions protocol. **D)** Individual learning curves of muscimol-treated (green, N=11) and vehicle-treated mice (gray, N=4) walking on the self-paced running wheel, with superimposed average %CR. p-value = 0.0208 from S6-14. p-values for M1 = 0.2986 and for E1-E4 = 0.7480. **E)** Individual eyelid closure of muscimol-treated (green, N=11) and vehicle-treated mice (gray, N=4) learning on the self-paced running wheel, with superimposed average %CR. p-value = 0.0017 from S7-14. p-values for M1 = 0.2685 and for E1-E4 = 0.7188. **F)** Average eyelid closure for CS-only trials of the last learning session (S14). Green lines represent the muscimol group, and gray lines the vehicle treated group. p-value = 0.0497. p-values for M1 = 0.2685 and for E1-E4 = 0.7188. **G)** Individual learning curves of muscimol treated animals (N=5), after completing the acquisition phase (as vehicle-treated mice, trained on the self-paced running wheel), with superimposed average %CR. **H)** Individual learning curves of muscimol-treated (green, N=7) and vehicle-treated mice (gray, N=6) running on the medium speed (0.10 m/s) motorized running wheel, with superimposed average %CR. p-value = 0.6208 from S5-14. p-values for M1 = 0.7316 and for E1-E4 = 0.8035. **I)** Individual eyelid closure of muscimol-treated (green, N=6) and vehicle-treated mice (gray, N=7) learning on the motorized running wheel (medium speed, 0.10 m/s), with superimposed average %CR. p-value = 0.1347 from S6-14. p-values for M1 = 0.6136 and for E1-E4 = 0.7744. **J)** Average eyelid closure for CS-only trials of the last learning session (S10). Green lines represent the muscimol group, and gray lines the vehicle treated group. p-value = 0.0.7738. Shaded error bars represent the standard error of the mean (SEM). *p<0.05, **p<0.01, ***p<0.001 and ns, not significant.

sessions of learning. For that, we trained WT mice on a motorized running wheel rotating at a fixed speed (0.10 m/s; medium speed). We first did this experiment in sessions with the same length as the ones from the self-paced running wheel (100 trials), and we did not observe any differences between the groups (data not shown). Thus, we decided to decrease the length of the session to 40 trials, aiming to slow down the learning and increase the likelihood of targeting the memory consolidation process. Surprisingly, the same post-session infusions of muscimol (as Figure 3.1 D) did not affect consolidation when mice were running at a constant speed: there were no differences between the experimental (N=7) and control (N=6) groups (Figure 3.1 H-J).

After the acquisition phase, the location of the guide cannula was confirmed by the decrease in learned responses observable in M1 (M1; Figure 3.1 shaded green bar). No differences between the two groups were observed neither in M1 nor in the extinction phase (Figure 3.1 H, I).

These results suggest that running makes memory consolidation less susceptible to post-session muscimol-dependent cortical inactivation.

3.1.3 Consolidation of eyeblink conditioning responses is not enhanced by post-session locomotion on the motorized running wheel

We next asked whether the lack of effect from post-session muscimol infusions observed in mice learning on the motorized running wheel (Figure 3.1 H) was caused by: a) the post-session running that occurs while animals are receiving their infusions (15 min duration) or b) by locomotion during the session itself. To investigate this, we performed a control experiment where mice were trained on the self-paced and then transferred to the motorized running wheel for the infusion protocol (Figure 3.2 A, B). If the result was to be more similar to the one of the motorized running wheel (no difference between muscimol and controls, Figure 3.1 H), then the running after the session, during the infusion process, was the primary factor responsible for the enhancement of consolidation. On the other hand, if the result was more similar to the self-paced running wheel (difference between muscimol and controls, Figure 3.1 D), then the running post-session was not the crucial factor for this process.

We observed a difference in learning rate between the two groups (muscimol N=5, vehicle

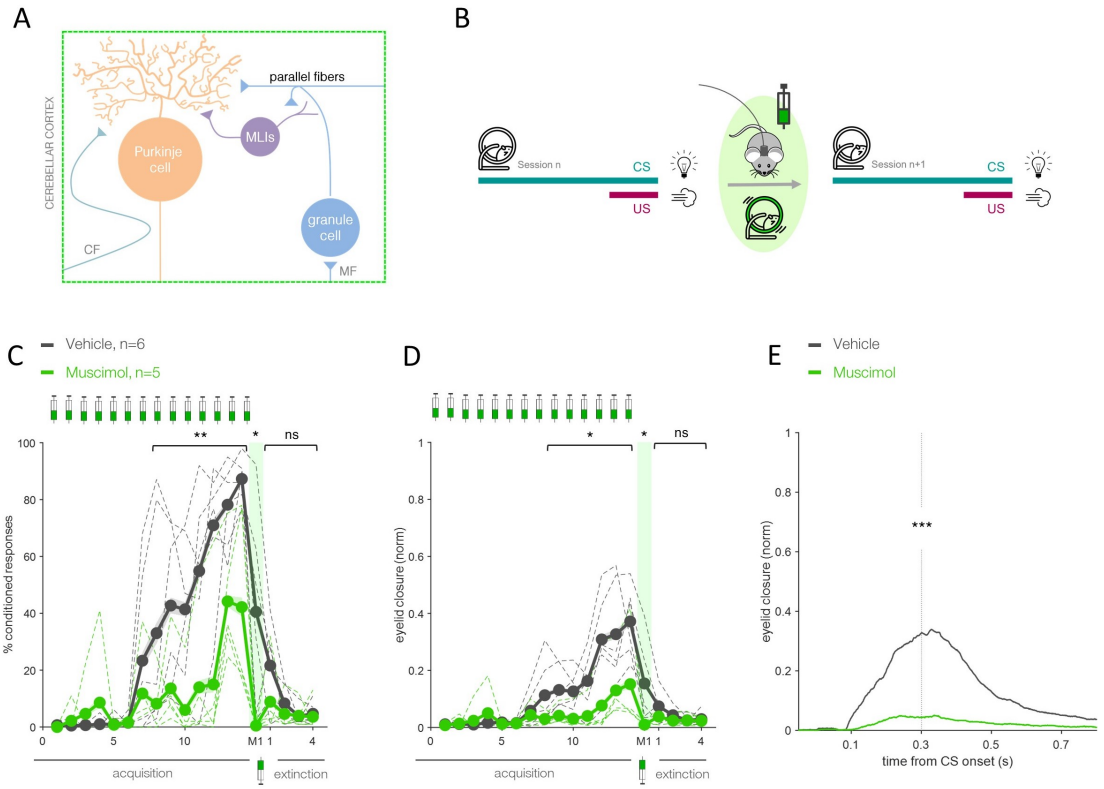

Figure 3.2: Post-session running activity is not responsible for the reduced susceptibility of eyeblink learned responses to post-session reversible inactivations of the cerebellar cortex on the motorized running wheel. To assess the importance of running during the infusion protocol, after performing the learning session on the self-paced running wheel, mice were transferred to the motorized running wheel for the post-session infusion protocol. **A)** Cerebellar circuit diagram representing the cerebellar cortex (dashed green square) as the target area for muscimol infusions. **B)** Schematics of training on the self-paced running wheel and post-session muscimol infusion while on the motorized running wheel. **C)** Individual learning curves of muscimol-treated (green, N=5) and vehicle-treated animals (gray, N=5), with superimposed average %CR. p-value = 0.0051 from S8-14. p-values for M1 = 0.0318 and for E1-E4 = 0.3516. **D)** Individual eyelid closure of muscimol-treated (green, N=5) and vehicle-treated mice (gray, N=6), with superimposed average %CR. p-value = 0.0145 from S9-14. p-values for M1 = 0.0464 and for E1-E4 = 0.2364. **E)** Average eyelid closure for CS-only trials of the last learning session (S14). Green lines represent the muscimol group, and gray lines the vehicle treated group. p-value = 0.0005. Shaded error bars represent the standard error of the mean (SEM). *p<0.05, **p<0.01, ***p<0.001 and ns, not significant.

N=6) (Figure 3.2 C-D) that was similar to the self-paced running wheel result. Thus, running during the session, and not after, appears to be the main driver of the locomotion modulation in motor memory consolidation.

We have also confirmed the appropriate location of the guide cannula with the M1 test (M1; Figure 3.2 A shaded green bar) and did not observe any differences in extinction rate between the groups (Figure 3.2 C). Mice from the muscimol-treated group appear to have a more abrupt decrease in CRs in M1, compared to littermate controls, but no differences were observed in the extinction phase (Figure 3.2 C, D).

Taken together, these results indicate that, similarly to the positive modulation of locomotion on the acquisition of eyeblink conditioning (Albergaria et al., 2018), running may also be enhancing the motor memory consolidation process.

3.2 Optogenetic perturbation of the cerebellar cortex

One hypothesis that emerges from the reversible inactivation results is that locomotor activity may promote a shift of the critical time window for consolidation of the eyeblink learned responses. The null effect of the post-session muscimol infusions when animals were engaged in locomotor activity during learning (Figure 3.1 H), suggests that memory consolidation might be happening in between the trial of each session, instead of only after it.

To further investigate the dynamics of memory consolidation of eyeblink conditioning responses, we took advantage of optogenetic fine temporal properties to perturb the cerebellar cortex. GCs, located in the cerebellar cortex, are a major excitatory input to PCs and have been previously implicated in memory consolidation of another cerebellar-dependent learning task (Galliano et al., 2013). Thus, to better determine the temporal properties of motor memory consolidation, we performed experiments to either stimulate or inhibit GCs' activity at specific time points during or after each learning session.

3.2.1 Optogenetic perturbation of GC during the ITI interferes with learning when animals are engaged in locomotor activity

To investigate if the time in between the learning trials was relevant for the consolidation of eyeblink responses when animals were engaged in locomotion, we trained mice on the motorized running wheel (0.10 m/s; medium speed) and optogenetically perturbed this period. Hence, we used mice expressing either ChR2 or ArchT under a GC-specific promoter, GC-ChR2 and GC-ArchT respectively, to optogenetically stimulate or inhibit GCs during the ITI (Figure 3.3 A-C).

Optogenetic stimulation of GCs during the ITIs delayed mice's learning (GC-ChR2 N=3) when compared to littermate controls (GC-CTL N=4) (Figure 3.3 D), indicating the importance of GCs' activity during the ITI period. This perturbation also led to a decrease in the amplitude of GC-ChR2 mouse responses (Figure 3.3 E, F).

Considering that the ChR2 stimulation electrically induces changes at the cellular level that

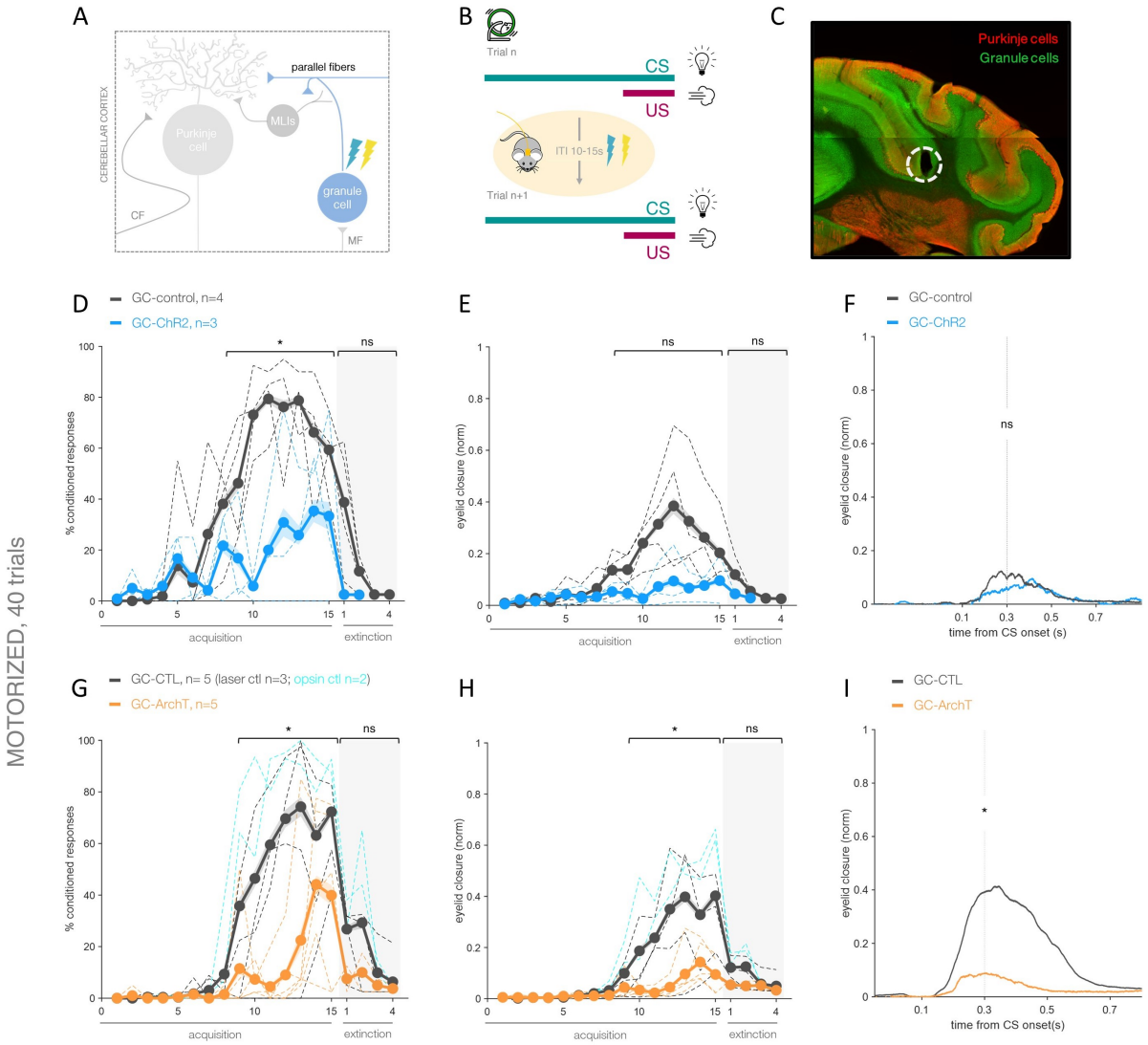

Figure 3.3: Optogenetic perturbation of GCs in between the trials of eyeblink conditioning affects learning of mice actively engaged in locomotor activity. To investigate the temporal dynamics of memory consolidation of eyeblink conditioning responses, we took advantage of optogenetic fine temporal properties to perturb the cerebellar cortex during the session, while mice were actively walking. **A)** Cerebellar circuit diagram representing the cerebellar cortex as the target of the optogenetic manipulations. Blue and yellow lighting bolts represents the specific cell target of laser stimulation or inhibition, respectively: granule cells. **B)** Schematics of intertrial interval (ITI) optogenetic perturbations protocol. **C)** Representative fluorescence image of a coronal cerebellar slice showing the optogenetic fiber track in the eyelid sulcus of the cerebellar cortex. **D)** Individual learning curves of GC-ChR2 (blue, N=3) and GC-CTL mice (gray, N=4) learning on the motorized running wheel (0.10 m/s) in 40-trial sessions, with superimposed average %CR. p-value = 0.0241 from S8-15. p-values for E1-E4 = 0.4253. **E)** Individual eyelid closure of GC-ChR2 (blue, N=3) and GC-CTL mice (gray, N=4) learning on the motorized running wheel (0.10 m/s) in 40-trial sessions, with superimposed average amplitude of CRs. p-value = 0.0834 from S8-15. p-values for E1-E4 = 0.5756. **F)** Average eyelid closure for CS-only trials of the last learning session (S15). Blue lines represent the experimental group, and gray lines the control group. p-value = 0.4773. **G)** Individual learning curves of GC-ArchT (orange, N=5) and GC-CTL mice (gray, N=6 , with opsin control mice in blue dashed lines (N=2)) learning on the motorized running wheel (0.10 m/s) in 40-trial sessions, with superimposed average %CR. p-value = 0.0305 from S9-15. p-values for E1-E4 = 0.1024. **H)** Individual eyelid closure of GC-ArchT (orange, N=5) and GC-CTL mice (gray, N=5 , with opsin control mice in blue dashed lines (N=2)) learning on the motorized running wheel (0.10 m/s) in 40-trial sessions, with superimposed average amplitude of CRs. p-value = 0.0181 from S10-15. p-values for E1-E4 = 0.0945. **I)** Average eyelid closure for CS-only trials of the last learning session (S15). Orange lines represent the experimental group, and gray lines the control group. p-value = 0.0267. Shaded error bars represents standard error of the mean (SEM). *p<0.05, **p<0.01, ***p<0.001 and ns, not significant.

are not visible at the behavioral level (Albergaria et al., 2018), we repeated the same protocol with GC-ArchT mice instead. We observed the same result as with GC-ChR2 mice: optogenetic inhibition of GCs also impairs learning (GC-ArchT N=5), comparing with littermate controls (GC-CTL N=6) (Figure 3.3 G-I). Thus, independently of the type of perturbation - stimulation (ChR2) or inhibition (ArchT) - the results were identical. These indicate again the importance of the ITI period in the consolidation of the eyeblink learned responses when animals are engaged in locomotion. No differences between the two groups were observed in the extinction phase (Figure 3.3 D, E, G and H).

These results were obtained from short sessions (40 trials) to compare with the results from the reversible inactivation on the motorized running wheel (Figure 3.1 H), where we aimed to increase the likelihood of targeting the consolidation process upon post-session infusions. However, if in the case where animals are engaged in locomotor activity the consolidation process is occurring mainly during the ITI period, the effect of the ITI perturbation should be independent of the number of trials in each session. Thus, and to be able to compare with the reversible inactivation on the self-paced running wheel, we performed the same protocol of ITI perturbation in longer sessions of 100 trials. We have also observed a tendency of the ITI optogenetic disruption, either stimulation or inhibition, to impair learning of eyeblink conditioning under these conditions, although at a smaller scale than in the shorter sessions (GC-ChR2 N=3, GC-CTL N=8; GC-ArchT N=3, GC-CTL N=2) (Figure 3.4). GCs may find a compensatory mechanism or a faster way to counteract the perturbation, as most animals eventually learn to comparable levels to the controls. No differences between the two groups were observed in the extinction phase (Figure 3.3 C, D, F and G).

Additionally, in some of the experiments, we also included two types of littermate controls. Mice that didn't express the opsin (either ChR2 or ArchT) but still received laser during the ITIs, to control for the light of the laser - laser CTL -, and mice that expressed the opsins but didn't receive laser during the ITI - opsin CTL -, to control for the effect of the expression of the opsins. We observed that opsin CTL animals learned identically to laser CTL animals (Figure 3.3 G, blue dashed lines; and Figure 3.4 C, yellow dashed lines).

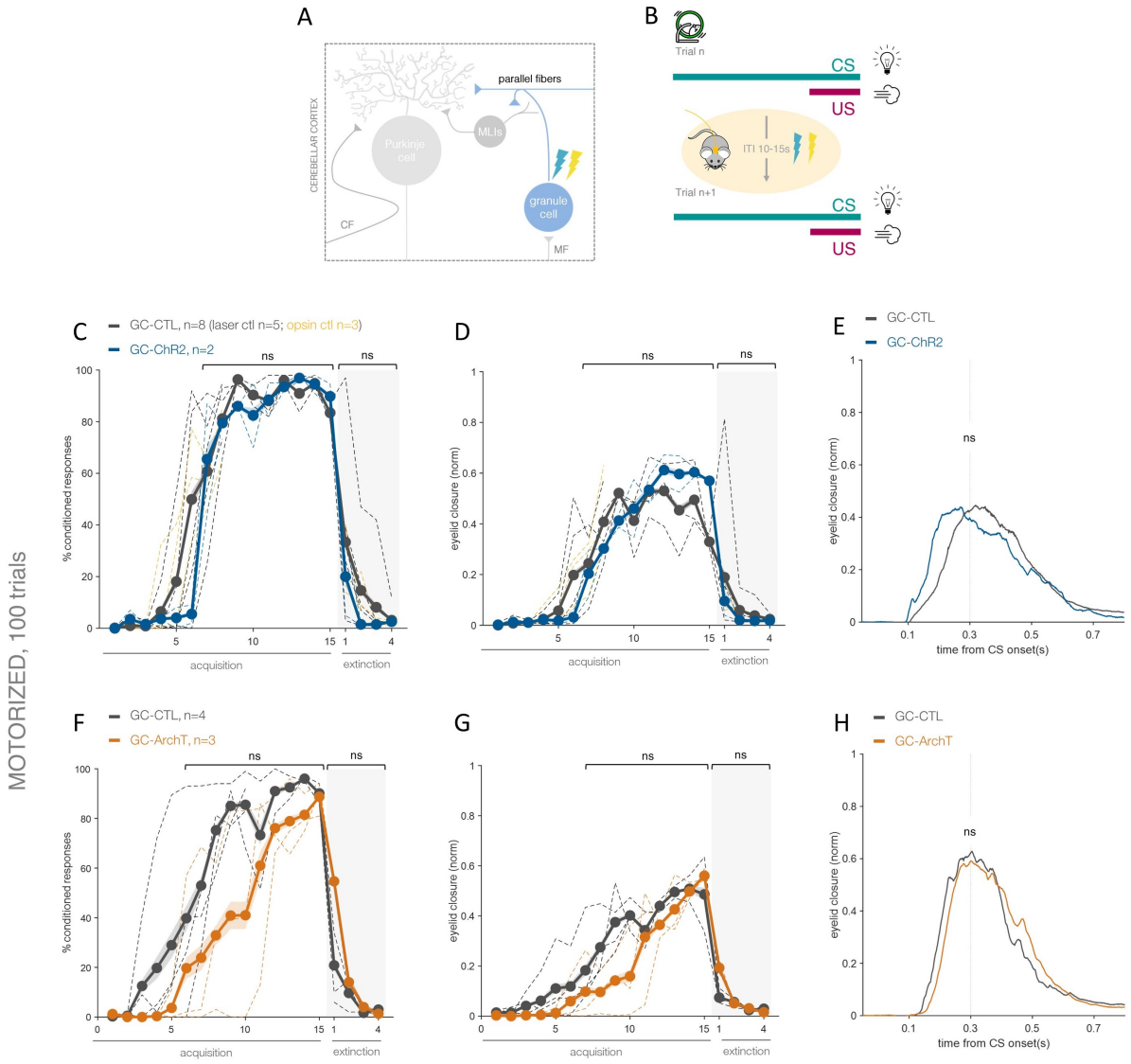

Figure 3.4: Optogenetic perturbation of GCs in between the trials of eyelid conditioning has less effect on learning in longer sessions. To further investigate the temporal dynamics of memory consolidation of eyeblink conditioning responses, we perturbed GC activity in between the trials of longer eyeblink learning sessions. **A)** Cerebellar circuit diagram representing the cerebellar cortex as the target of the optogenetic manipulations. Blue and yellow lighting bolts represents the specific cell target of laser stimulation or inhibition, respectively: granule cells. **B)** Schematics of intertrial interval (ITI) optogenetic perturbations protocol. **C)** Individual learning curves of GC-ChR2 (dark blue, N=2) and GC-CTL mice (gray, N=8, with opsin control mice (yellow dashed lines, N=3)), learning on the motorized running wheel (0.10 m/s) in 100-trial sessions, with superimposed average %CR. p-value = 0.6208 from S6-15. p-values for E1-E4 = 0.2957. **D)** Individual eyelid closure of GC-ChR2 (dark blue, N=2) and GC-CTL mice (gray, N=8, with opsin control mice (yellow dashed lines, N=3)), learning on the motorized running wheel (0.10 m/s) in 100-trial sessions, with superimposed average amplitude of CRs. p-value = 0.3507 from S6-15. p-values for E1-E4 = 0.3179. **E)** Average eyelid closure for CS-only trials of the last learning session (S15). Dark blue lines represent the experimental group, and gray lines the control group. p-value = 0.3865. **F)** Individual learning curves of GC-ArchT (dark orange, N=3) and GC-CTL mice (gray, N=4) learning on the motorized running wheel (0.10 m/s) in 100-trial sessions, with superimposed average %CR. p-value = 0.3560 from S5-15. p-values for E1-E4 = 0.4873. **G)** Individual eyelid closure of GC-ArchT (dark orange, N=3) and GC-CTL mice (gray, N=4) learning on the motorized running wheel (0.10 m/s) in 100-trial sessions, with superimposed average amplitude of CRs. p-value = 0.6247 from S7-15. p-values for E1-E4 = 0.5510. **H)** Average eyelid closure for CS-only trials of the last learning session (S15). Dark orange lines represent the experimental group, and gray lines the control group. p-value = 0.4084. Shaded error bars represents standard error of the mean (SEM). *p<0.05, **p<0.01, ***p<0.001 and ns, not significant.

3.2.2 Optogenetic perturbation of GC during the ITI does not affect learning when mice are voluntarily walking on the self-paced running wheel

To check whether consolidation in the self-paced is mainly post-session, as suggested by the muscimol infusion results (Figure 3.1 D), we performed the same ITI optogenetic perturbations (as Figures 3.3 and 3.4) but while animals were walking on the self-paced running wheel, instead of the motorized (Figure 3.5 A, B). In the case consolidation of eyeblink conditioning for mice learning on this condition is mainly post-session, then the perturbation during the ITIs should not yield an effect.

In agreement with our prediction, we observed that perturbation of the ITI period of animals learning on the self-paced running wheel does not affect consolidation. Both control and experimental animals, either with laser stimulation or inhibition, had comparable learning performances (GC-ChR2 N=3, GC-CTL N=2; GC-ArchT N=3, GC-CTL N=4) (Figure 3.5 C-H). No differences between the two groups were observed in the extinction phase (Figure 3.3 C, D, F and G).

This result suggests that consolidation on the self-paced running wheel occurs mainly post-session, as expected, confirming our reversible inactivation results (Figure 3.1 D) and previous literature (Attwell et al., 2002; Cooke et al., 2004). Additionally, these results also showed that laser perturbation in between the learning trials did not affect the mice's ability to learn and/or express the learned responses in the ITI perturbation on the motorized running wheel (Figures 3.3 and 3.4).

The finding that GC optogenetic perturbation during the session, in between the trials, impairs learning of eyeblink conditioning on the motorized running wheel but not on the self-paced running wheel provides further evidence that running activity enhances motor memory consolidation, perhaps by shifting its time window to within the session. It also raises the possibility that GCs might be differentially recruited during the eyeblink memory consolidation process depending on the mouse's locomotor activity.

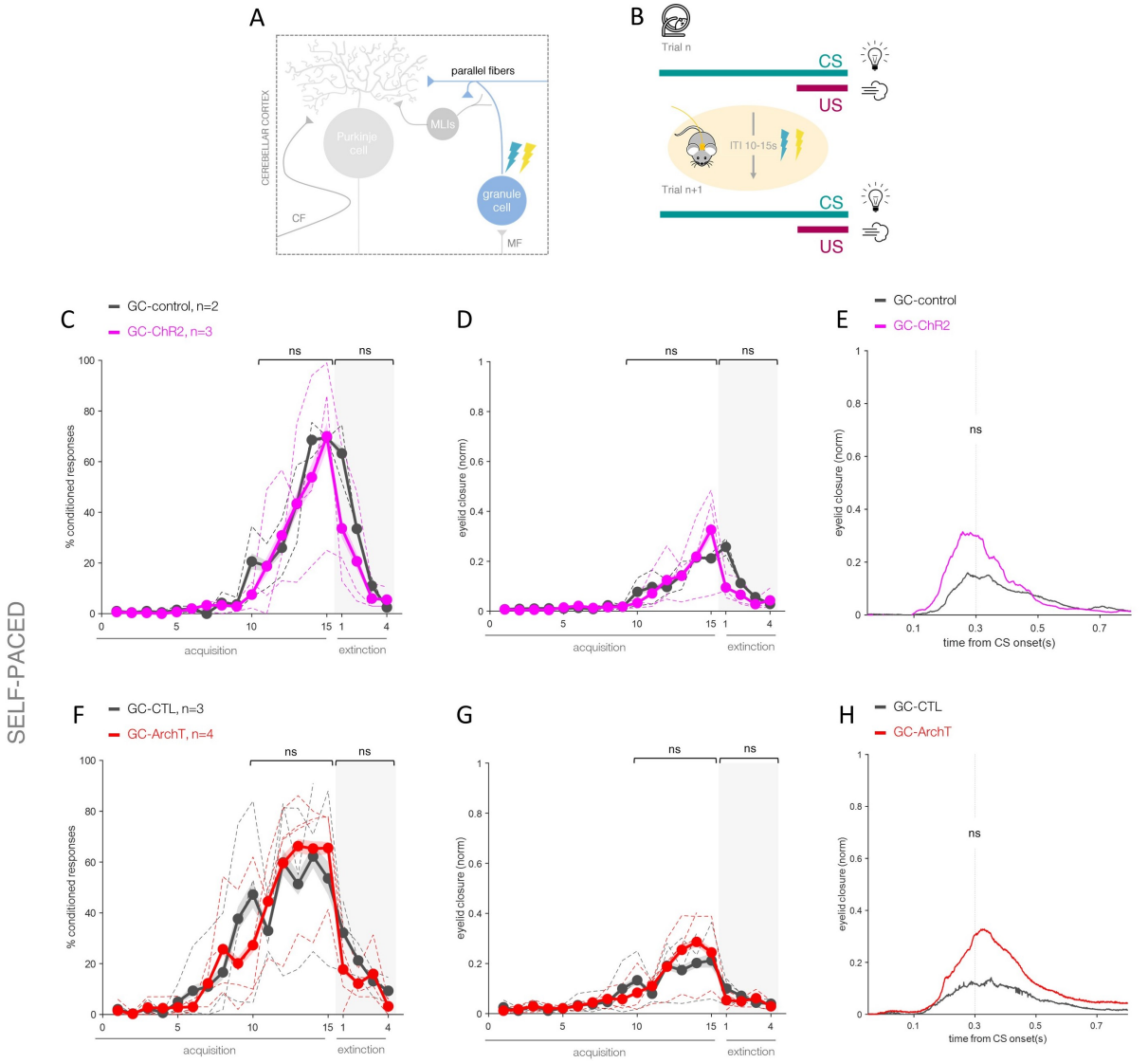

Figure 3.5: Optogenetic perturbation of GCs in between the trials of eyeblink conditioning does not affect the learning of mice walking voluntarily. As a control to the laser stimulation and to verify whether consolidation on the self-paced is mainly post-session, we performed the ITI optogenetic perturbations while animals were walking on the self-paced running wheel. **A)** Cerebellar circuit diagram representing the cerebellar cortex as the target of the optogenetic manipulations. Blue lighting bolt represents the specific cell target of laser stimulation: granule cells. **B)** Schematics of intertrial interval (ITI) optogenetic perturbations protocol. **C)** Individual learning curves of GC-ChR2 (pink, N=3) and GC-CTL mice (gray, N=4) learning on the self-paced running wheel, with superimposed average %CR. p-value = 0.9221 from S12-15. p-values for E1-E4 = 0.4914. **D)** Individual eyelid closure of GC-ChR2 (pink, N=3) and GC-CTL mice (gray, N=2) learning on the self-paced running wheel, with superimposed average amplitude of CRs. p-value = 0.8793 from S10-15. p-values for E1-E4 = 0.3358. **E)** Average eyelid closure for CS-only trials of the last learning session (S15). Pink lines represent the experimental group, and gray lines the control group. p-value = 0.5030. **F)** Individual learning curves of GC-ArchT (red, N=5) and GC-CTL mice (gray, N=6) learning on the self-paced running wheel, with superimposed average %CR. p-value = 0.9572 from S9-15. p-values for E1-E4 = 0.3076. **G)** Individual eyelid closure of GC-ArchT (red, N=2) and GC-CTL mice (gray, N=2) learning on the self-paced running wheel, with superimposed average amplitude of CRs. p-value = 0.8371 from S9-15. p-values for E1-E4 = 0.3672. **H)** Average eyelid closure for CS-only trials of the last learning session (S15). Red lines represent the experimental group, and gray lines the control group. p-value = 02488. Shaded error bars represents standard error of the mean (SEM). *p<0.05, **p<0.01, ***p<0.001 and ns, not significant.

3.2.3 Post-session optogenetic perturbation affects consolidation in mice learning on the self-paced but not on the motorized running wheel

As a complementary experiment to understand whether optogenetic stimulation of GCs after each session of learning would produce the same effect as muscimol post-session infusions (Figure 3.1 D, H), we optogenetically perturbed the post-session period, both on the self-paced and motorized running wheels (Figure 3.6 A, B).

Strikingly, 10 min of interspersed laser stimulation of GCs (for 5 s every 10 to 15 s, randomized) after each learning session while mice were on the self-paced running wheel was enough to delay the acquisition of their CRs (GC-ChR2 N=2), when comparing to littermate controls (GC-CTL N=2) (Figure 3.6 C-E). In contrast with post-session reversible inactivation, GC-ChR2 did not reach the same levels of learning as their control littermates (Figure 3.6 C-E). On the other hand, the same post-session laser perturbation did not yield the same effect on the consolidation of mice learning while engaged in locomotor activity (GC-ChR2 N=3, GC-CTL N=3) (Figure 3.6 F-H). No differences between the two groups were observed in the extinction phase (Figure 3.6 C, D, F and G).

By using a more temporally precise technique that affects GCs specifically, we obtained results in line with the muscimol reversible inactivation of the cerebellar cortex (Figure 3.1 3.1), confirming the temporal discrepancy of the motor memory consolidation window depending on locomotor engagement during task performance.

3.2.4 Optogenetic perturbation during the ITI does not seem to affect mice's ability to express their eyeblink learned responses

To assess if laser perturbation during the ITI was affecting learning processes other than consolidation, we performed a test at the end of the acquisition phase (Figure 3.7 A-C). This test consisted of blocks without laser followed by blocks with laser perturbation in between the trials (test blocks), to a total of 6 or 10 blocks, for short or long protocols, respectively. In the case laser perturbation in between the trials was somehow impairing the cells' ability to

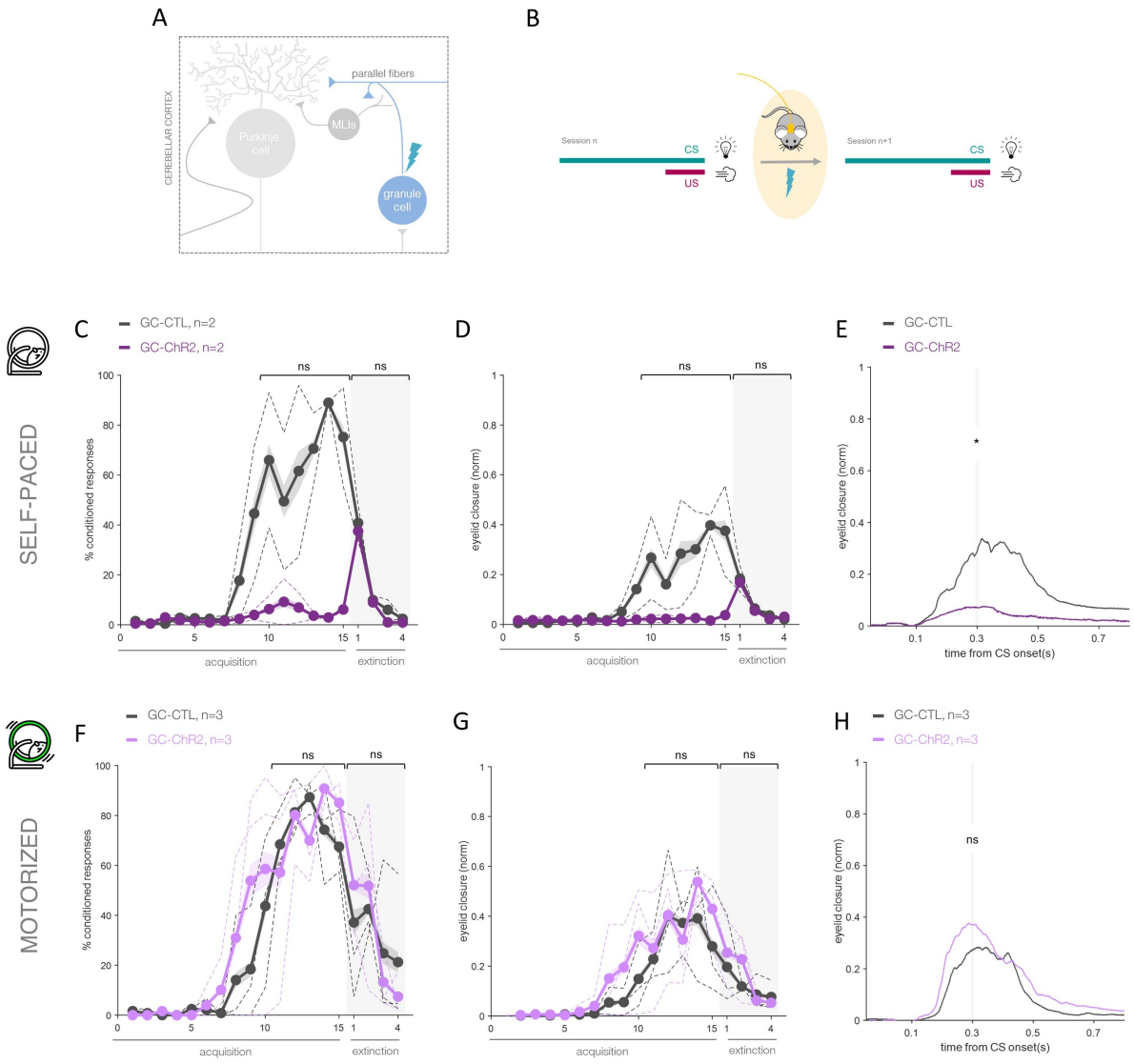

Figure 3.6: Post-session optogenetic perturbation of GCs only affects eyeblink conditioning of mice that are not engaged in locomotion during the session. To understand whether post-session optogenetic perturbation would produce the same effect as post-session infusions, we optogenetically stimulated GCs after each session of learning, on both the self-paced and motorized running wheels. **A)** Cerebellar circuit diagram representing the cerebellar cortex as the target of the optogenetic manipulations. Blue lighting bolt represents the specific cell target of laser stimulation: granule cells. **B)** Schematics of post-session optogenetic perturbations protocol. **C)** Individual learning curves of GC-ChR2 (purple, N=2) and GC-CTL mice (gray, N=2) learning on the self-paced running wheel, with superimposed average %CR. p-value = 0.1108 from S9-15. p-values for E1-E4 = 0.8359. **D)** Individual eyelid closure of GC-ChR2 (purple, N=3) and GC-CTL mice (gray, N=2) learning on the self-paced running wheel, with superimposed average amplitude of CRs. p-value = 0.2045 from S9-15. p-values for E1-E4 = 0.8921. **E)** Average eyelid closure for CS-only trials of the last learning session (S15). Purple lines represent the experimental group, and gray lines the control group. p-value =0.0371. **F)** Individual learning curves of GC-ChR2 (lilac, N=3) and GC-CTL mice (gray, N=3) learning on the motorized running wheel (0.10 m/s) in 40-trial sessions, with superimposed average %CR. p-value = 0.8360 from S10-15. p-values for E1-E4 = 0.9841. **G)** Individual eyelid closure of GC-ChR2 (lilac, N=3) and GC-CTL mice (gray, N=3) learning on the motorized running wheel (0.10 m/s) in 40-trial sessions, with superimposed average amplitude of CRs. p-value = 0.6056 from S10-15. p-values for E1-E4 = 0.6332. **H)** Average eyelid closure for CS-only and CS-US trial traces of the last learning session (S15). Lilac lines represent the experimental group, and gray lines the control group. p-value = 0.6219. Shaded error bars represent the standard error of the mean (SEM). *p<0.05, **p<0.01, ***p<0.001 and ns, not significant.

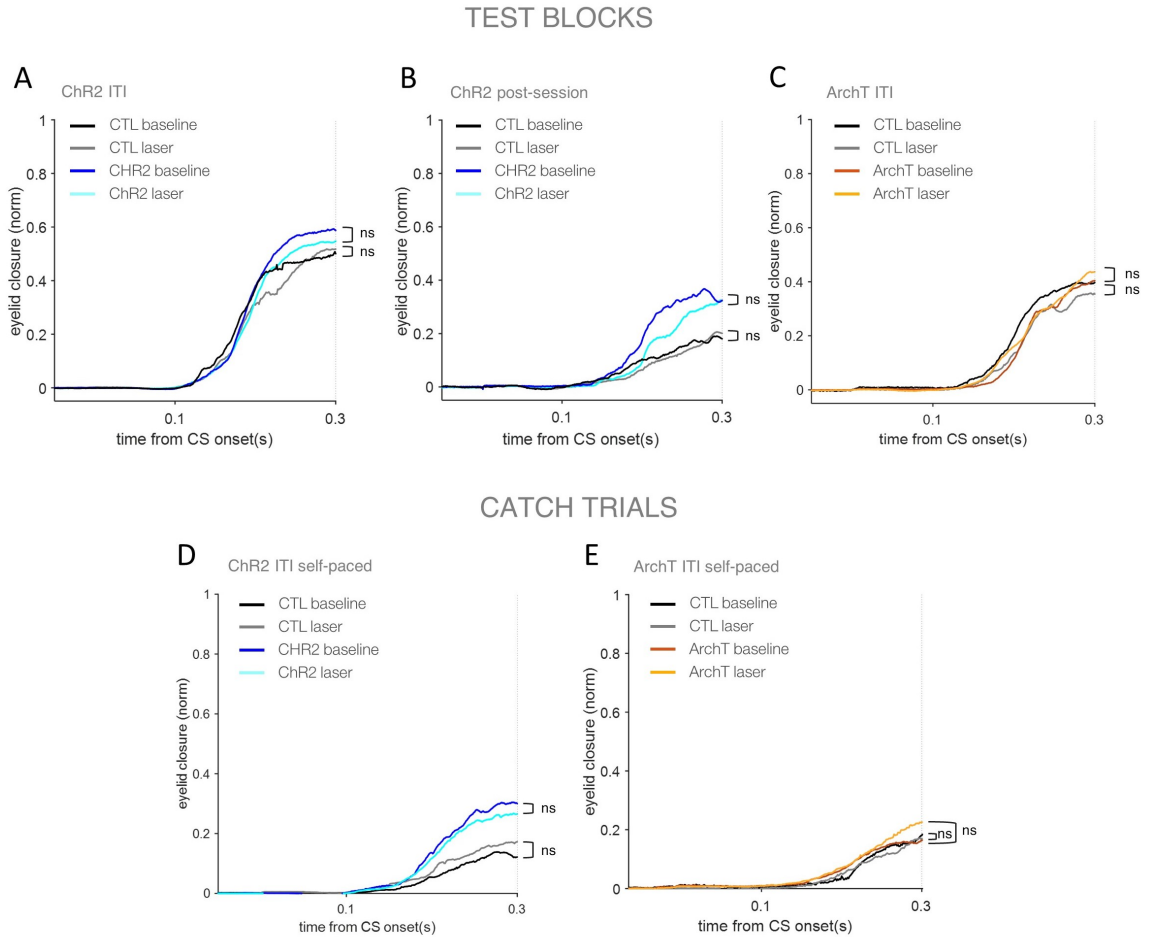

Figure 3.7: Optogenetic perturbation of GCs in between the trials does not affect the expression of eyeblink responses, independently of the stage of learning. To test if GCs perturbation impairs the cells ability to respond on the following trial, we have conducted test trials/sessions where we compare the amplitude of eyeblink learned responses after the presence or absence of laser perturbation, both during and after animals have learned. **A-C)** Average eyelid closure for CS-US trials (showing until US onset: 0.3 s after CS onset) from test blocks, for optogenetic perturbation during the ITI (A; CTL baseline vs laser, p-value = 0.9616; ChR2 baseline vs laser, p-value = 0.7827) and post-session (B ; CTL baseline vs laser, p-value = 0.9125; ChR2 baseline vs laser, p-value = 0.8156) using GC-ChR2 mice, and for optogenetic inhibition during the ITI using GC-ArchT mice (C; CTL baseline vs laser, p-value = 0.9407; ArchT baseline vs laser, p-value = 0.6827). Black and gray lines indicate average CRs on blocks of no laser presentation (baseline) and with laser perturbation in between the trials, for control animals. Dark blue and dark orange lines indicate average baseline CRs, and blue and orange lines indicate average CRs on blocks with laser presentation for perturbed mice (GC-ChR2 or GC-ArchT, respectively). **D, E)** Average eyelid closure for CS-US trials (showing until US onset: 0.3 s after CS onset) from catch trials, for optogenetic perturbation during the ITI for GC-ChR2 mice (D; CTL baseline vs laser, p-value = 0.1455; ChR2 baseline vs laser, p-value = 0.8515) and for GC-ArchT mice (E; CTL baseline vs laser, p-value = 0.7335; ArchT baseline vs laser, p-value = 0.7801) trained on the self-paced running wheel. Black and gray lines indicate average CRs on trials following no laser presentation (baseline) and trials following laser presentation, for control animals. Dark blue and dark orange lines indicate average baseline CRs, and blue and orange lines indicate average CRs on trials following laser presentation for perturbed mice (GC-ChR2 or GC-ArchT, respectively). Shaded error bars indicate standard error of the mean (SEM). *p<0.05, **p<0.01, ***p<0.001 and ns, not significant.

respond on the next trial, then blocks where no laser perturbation was delivered should exhibit enhanced learned responses. We verified that the CRs were not enhanced in blocks without the laser compared to the ones with the laser perturbation (Figure 3.7 A-C), for both stimulation (A, B) and inhibition (C) of GCs, indicating that in these experiments we were mainly targeting the consolidation process.

The test block was performed at the end of the acquisition phase when memory is considered to be more stable (Dudai, 2004). To test whether the cells' ability to respond appropriately had been impaired by laser perturbation throughout the acquisition phase, where memory is more labile, we have incorporated trials where no laser perturbation was delivered in the previous ITI - catch trials. Similar to the test block results, we did not observe any difference in the expression of the learned responses between a trial following ITI perturbation and a trial without it (Figure 3.7 D, E).

Both reversible inactivation and optogenetic perturbation results have provided solid evidence pointing in the direction of our main hypothesis that running makes the consolidation process faster, possibly by shifting its relevant time window to within the sessions of learning (Figure 3.8, summary table). Optogenetic perturbation of GCs during the session only perturbed animals actively walking during the task (A, C) and not the ones that were not (B, D). Whereas post-session perturbation of the cerebellar cortex's activity, using either muscimol infusions or optogenetic tools, affected consolodation on mice voluntarily walking during the task (F, H), and not the ones engaged in locomotion (E, G). Our results also highlight the importance of GCs for eyeblink memory consolidation in mice.

3.3 Exploring the potential shift in memory storage location enhanced by locomotion

The different cerebellar cortex perturbations that we have performed (Figures 3.8 A-D, G and H) have consistently pointed in the direction of a temporal shift in motor memory consolidation when mice are running during the eyeblink conditioning. Although locomotion seemingly prompts a shift of the time window for consolidation of eyeblink conditioning responses, there is also the possibility that it may induce an earlier spatial shift on memory storage - systems consolidation (Dudai, 2004). It has been proposed for another cerebellar-dependent learning

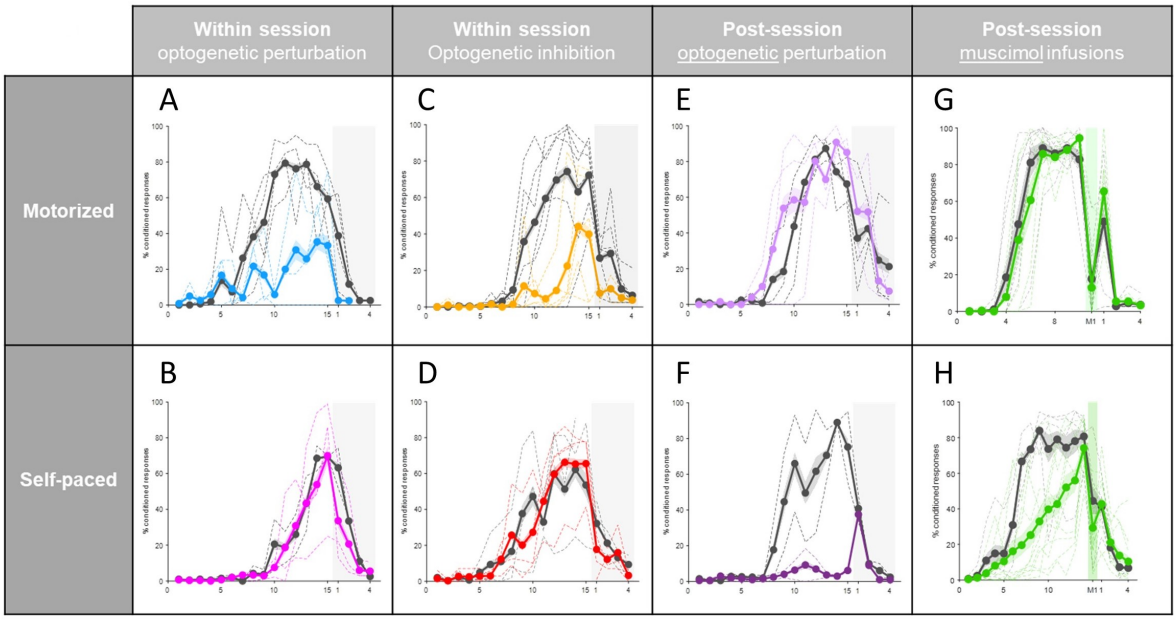

Figure 3.8: Summary – Double dissociation distinguishing within and post-session perturbations, and learning while on self-paced and motorized running wheels. Summary table showing the main results from perturbation of the cerebellar cortex's activity, from both reversible inactivation (right column; G, H) and optogenetic stimulation/inhibition (left panels; A-F). The table shows that post-session perturbations (E-H) only affect mice voluntarily walking during the session, and that within session perturbations (A-D) only affect animals engaged in locomotor activity during the session.

task that, after a given amount of time, memories that are initially formed in the cerebellar cortex are then "shifted" to other downstream regions, such as the DCN, which is the primary receiver from the cerebellar cortex (Kassardjian et al., 2005). In the eyeblink conditioning task, the required DCN for this process is the AIP (Krupa et al., 1993; Heiney et al., 2014; Brinke ten et al., 2017).

To investigate the spatial dynamics of cerebellar motor memories and dissect the mechanism for the consolidation of eyeblink conditioning, we conducted post-session reversible inactivations of the AIP.

3.3.1 Investigating a potential spatial shift in motor memory storage location, from the cerebellar cortex to the AIP, in the motorized running condition

As a first step towards investigating the possibility of a spatial shift on memory storage location, we aimed to test if the AIP was being recruited in the early stages of learning upon running activity. We trained two randomly assigned groups of mice to either receive muscimol (N=3) or vehicle post-session infusions (N=3), while they were on the motorized running wheel

(medium speed; 0.10 m/s), in a similar manner to the reversible inactivations of the cerebellar cortex (Figure 3.9 A-C).

We observed a small delay in the learning of the AIP muscimol-treated mice when compared to littermate controls (vehicle N=3, muscimol N=3) (Figure 3.9 D-F). Since muscimol infusions to the cerebellar cortex on mice learning on the motorized running wheel did not affect their consolidation (Figure 3.1 D), the difference observed in AIP experiments suggests a possible earlier involvement of this DCN structure in learning driven by locomotor activity.

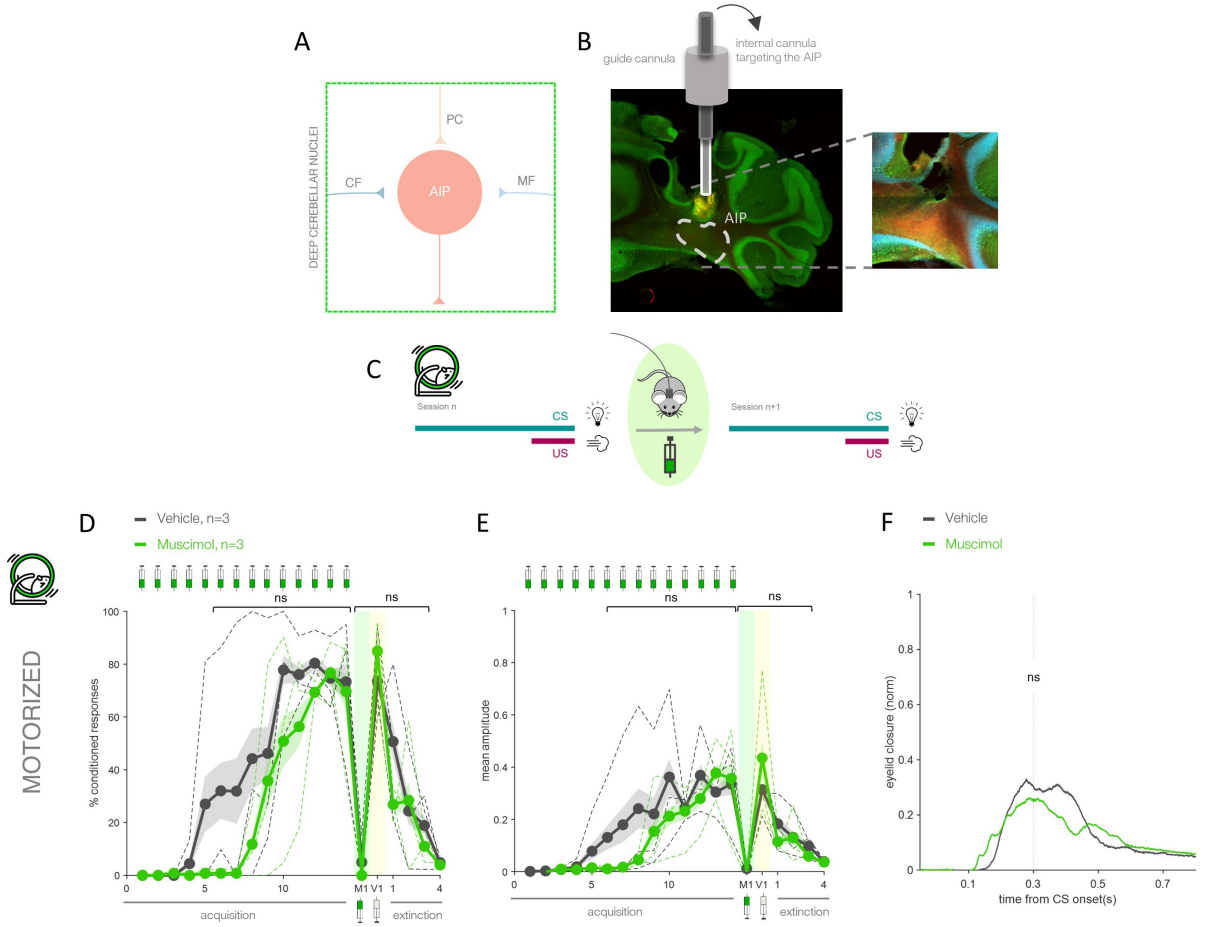

Figure 3.9: Post-session reversible inactivation of the AIP cerebellar nucleus induce a sublte delay in the learning of eyeblink conditioning, when mice are engaged in running activity. To investigate the spatial shift on memory storage due to running activity we conducted post-session reversible inactivation of the AIP while animals were engaged in locomotion. **A)** Cerebellar circuit diagram representing the AIP (dashed green square) as the target area for muscimol infusions. **B)** Representative fluorescence image of a coronal cerebellar slice showing the cannula track targeting the AIP and a close-up to the muscimol spread into the nucleus. Depicted in the figure is also the guide cannula implanted at the surface of the cerebellum through which the internal cannula is introduced to deliver the infusions to the AIP. **C)** Schematics of post-session muscimol infusions protocol. **D)** Individual learning curves of muscimol-treated (green, N=3) and vehicle-treated mice (gray, N=3) walking on the motorized running wheel (medium speed, 0.10 m/s), with superimposed average %CR. p-value = 0.4070 from S15-15. p-values for M1 = 0.3739, for V1 = 0.4367 and for E1-E4 = 0.5504. **E)** Individual eyelid closure of muscimol-treated (green, N=3) and vehicle-treated mice (gray, N=3), with superimposed average %CR. p-value = 0.5722 from S6-15. p-values for M1 = 0.3926, for V1 = 0.5401 and for E1-E4 = 0.4860. **F)** Average eyelid closure for CS-only trials of the last learning session (S14). Green lines represent the muscimol group, and gray lines the vehicle treated group. p-value = 0.7601. Shaded error bars indicate standard error of the mean (SEM). *p<0.05, **p<0.01, ***p<0.001 and ns, not significant.

At the end of the acquisition phase, we confirmed the correct location of the guide cannula through the observable decrease in learning performance (M1; Figure 3.9 D, shaded green bar),

since muscimol infusions to the AIP also affect the expression of CRs (Attwell et al., 2002; Heiney et al., 2014). Performance returned to normal values after doing the same test with vehicle ACSF infusions instead (V1; Figure 3.9 D, shaded yellow bar). No differences between the two groups were observed neither in M1, V1 nor in the extinction phase (Figure 3.9 D, E).

These preliminary data suggest that when mice are learning eyeblink conditioning while engaged in running activity there may also be a subtle spatial shift of the motor memory location, together with a temporal shift in the time window of motor memory consolidation. However, further experiments are needed to compare with the results from the self-paced running condition (Figure 3.1 D).

Chapter 4

Discussion

Memory consolidation has been described as a post-training process occurring on a scale of hours (Dudai, 2004). Yet, this description fits mostly declarative hippocampal-dependent memories. Other memory types, such as associative motor memories, might be mechanistically different and thus their consolidation may occur on a very different time scale.

Surprisingly, our results point in a new direction from previous studies of both declarative (Dudai et al., 2015) and motor memories (Attwell et al., 2002; Cooke et al., 2004; Robertson et al., 2004), opening the possibility of an adaptable time window for motor memory consolidation, driven by locomotion. Overall, our work suggests a faster motor memory consolidation process, on the order of seconds when animals are engaged in running during the learning task.

4.1 Running modulation

We have confirmed that the cerebellar cortex is required for the consolidation of learned eyeblink responses in mice (Attwell et al., 2002; Cooke et al., 2004), but the timescale for this process appears to be different when animals are engaged in locomotion (Figure 3.1). Exercise has been associated with the enhancement of attention, synaptic plasticity and learning (Smith et al., 2010; El-Sayes et al., 2019), however, studies about the effects of exercise in learning have been evaluated before or after the training sessions, but always dissociable from the learning task itself (Roig et al., 2012; Ferrer-Uris et al., 2017; Dal Maso et al., 2018). However, a positive relationship between running and cerebellar motor learning, specifically during the learning task, has recently been described (Albergaria et al., 2018). In line with this, here we have shown that locomotion during the learning task has a positive effect on the consolidation of

cerebellar motor memories (Figures 3.1 and 3.2).

Through the use of a temporally precise technique (optogenetics), we have further shown that memory consolidation may be happening in between the trials of the learning sessions, in the presence of modulation through running (Figure 3.3). Interestingly, a similar phenomenon was observed recently in a motor task performed by humans (Bönstrup et al., 2019). The authors found rapid motor skill improvements during the short intervals in between the learning trials, suggesting that consolidation could be happening in the timescale of seconds, similar to the timescale we have identified in our study.

As the period in between trials seems to be the main temporal window for consolidation in mice learning eyeblink conditioning while engaged in locomotion, it would be interesting to manipulate it to be outside the time range used in our study (ITI: 10-15 s). By using shorter ITIs of 1-5 s or longer ITIs of 20-25 s, and measuring their effects on eyeblink conditioning performance one could evaluate if these manipulations yield similar results to the optogenetic perturbation of GCs activity presented here (Figure 3.3), further investigating the importance of these intervals, and how they are influenced by running activity.

4.2 Possible neuronal mechanism for faster motor memory consolidation promoted by running - temporal shift

Our results suggest that being engaged in locomotion during the learning task enhances the consolidation of eyeblink learned responses and that GCs seem to be involved in this process (Figures 3.3, 3.4, 3.5 and 3.6). There are several possibilities to the underlying mechanisms by which running promotes motor memory consolidation. One possibility is an overall faster integration of sensory stimuli being driven by running activity (Niell, Stryker, 2010; Ayaz et al., 2013). In line with this possibility, it could also be that the multimodal integration of both running and CS input brings GCs closer to the threshold to fire and thus respond strongly, enhancing the learning responses, as seen before (Ishikawa et al., 2015; Powell et al., 2015; Albergaria et al., 2018). However, these possibilities only account for running modulation during the trials of learning, and our results suggest that GCs activity in between the trials is the main promoter of motor memory consolidation. Therefore, other possibilities are that more GCs

are being recruited and/or that GCs are becoming more active due to running activity (Ozden et al., 2012), perhaps in between the trials of the learning session. Maybe even exhibiting pattern repetition of the engram formed during the learning trials, as it has previously been described (Liu et al., 2012; Ramanathan et al., 2015).

As optogenetic experiments with ChR2 stimulation entail caveats like the possibility of the introduction of a new signal perhaps able to create a new pattern of neural activity, we have also performed experiments using ArchT inhibition, which provides an alternative approach. We have observed the same results with both ChR2 stimulation and ArchT inhibition of GCs (Figures 3.3, 3.4 and 3.5). Furthermore, the fact that we observed different results when performing the same optogenetic perturbations while only varying the running (Figure 3.3 vs 3.5 and Figure 3.6 C vs F), points in the direction of a specific perturbation of memory consolidation. To further confirm that these manipulations were specific to memory consolidation, we also performed test blocks and catch trials (Figure 3.7); so far only for the self-paced but in the future also for the motorized conditions.

Given the relevance of GCs for the consolidation of eyeblink learned responses, in the future we would like to perform calcium-imaging of GCs activity using a two-photon microscope: during the trial, in between the trials and post-session; while animals are engaged in running vs not. This would help us decipher how differentially active GCs are at different periods of the learning session, and how running modulates GCs activity.

Although our (Figures 3.3, 3.4, 3.5 and 3.6) and previous results (Galliano et al., 2013) indicate that GCs are important for the motor memory consolidation process, it is not yet clear what their exact contribution is. Due to inherent cerebellar circuit properties, GCs activity influences the activity of other cells downstream including MLIs and PCs. Therefore, to evaluate the specific contribution of GCs in this process, we will also conduct experiments where we manipulate the activity of either MLIs or PCs during the relevant time window for consolidation. By comparing these results with the ones of GCs perturbation, we will be able to dissect the circuit underlying cerebellar motor memory consolidation, and how it is modulated by running.

4.3 Possible spatial shift of cerebellar motor memory storage location

The main focus of this project was the study of the temporal dynamics of motor memory consolidation, and we have observed a faster/earlier temporal window for the memory consolidation process when animals are engaged in locomotion. However, besides the shift in the memory consolidation time window, our preliminary results also suggest the possibility of an earlier shift of the memory storage location from the cerebellar cortex to the AIP cerebellar nucleus being driven by running activity (Figure 3.9). As locomotion increases MF activity (Powell et al., 2015), this could potentially lead to increased synaptic plasticity between MF-AIP upon running activity, possibly recruiting this area in an earlier learning phase.

A critical next step, to appropriately evaluate the possible early recruitment of the AIP when mice are engaged in locomotion, will be the use of different perturbations on different running conditions. We will do so by performing both pharmacological reversible inactivations of the AIP and also optogenetically inhibiting its activity via stimulation of PCs axons, which are located in the AIP cerebellar nucleus. By performing neuronal manipulation at different time scales, these approaches will allow us to explore the involvement of this area at different time periods during learning. Additionally, it would also be interesting to see if the inhibition of the AIP would induce different results depending on the learning stage of the animals.

4.4 Novel consolidation mechanism for cerebellar motor memories

Our main objective with this thesis was to understand the dynamics of cerebellar motor memory consolidation. There is a large body of literature for declarative hippocampal-dependent memory consolidation, however, knowledge on how motor memories are consolidated is still poorly understood. In general, memories are thought to be consolidated post-training and benefit from post-training sleep and exercise (Dudai, 2012; Dudai et al., 2015; Ferrer-Uris et al., 2017). Procedural memory consolidation is mostly described as an offline motor skill gain, which refers to post-training processes on the order of hours to days (Robertson et al., 2004). However, results from a recent study (Bönstrup et al., 2019), suggest that these motor

skill gain improvements are taking place on a much faster scale, during the brief resting periods in between the learning trials (in the order of seconds). Overall, in line with this recent evidence, our results indicate that the consolidation time window for cerebellar-dependent memories could be dynamically changed depending on internal state modulation, in particular engagement in locomotion during the learning task (Figure 3.8). Thus, the memory consolidation process may have different temporal and spatial properties depending on the learning task and the brain areas involved. Our results extend the concept of memory consolidation from a post-training process, taking hours to days and being dependent on post-session sleep and exercise, to an adaptable process driven by running activity that occurs in the seconds in between the trials while the subjects are performing the learning task.

4.5 Conclusion

We have performed several experiments exploring how cerebellar motor memories are consolidated, aiming to understand their temporal and spatial properties. Our results point in the direction of a novel faster consolidation time window that can be dynamically regulated by locomotor activity. In the future, we will continue to investigate the neuronal mechanisms underlying the consolidation of eyeblink learned responses by evaluating the changes in temporal and spatial features driven by running modulation.

Bibliography

Albergaria Catarina, Silva N. Tatiana, Pritchett Dominique L., Carey Megan R. Locomotor activity modulates associative learning in mouse cerebellum // Nature Neuroscience. 2018. 21, 5. 725–735.

Albus J. S. A Theory of Cerebellar Function // Mathematical Biosciences. 1971. 10. 25–61.

Antonietti Alberto, Casellato Claudia, D'Angelo Egidio, Pedrocchi Alessandra. Model-driven analysis of eyeblink classical conditioning reveals the underlying structure of cerebellar plasticity and neuronal activity // IEEE Transactions on Neural Networks and Learning Systems. 2017. 28, 11. 2748–2762.

Attwell Phillip J.E., Cooke Samuel F., Yeo Christopher H. Cerebellar Function in Consolidation of a Motor Memory // Neuron. 2002. 34, 6. 1011–1020.

Ayaz Asli, Saleem Aman B., Schölvinck Marieke L., Carandini Matteo. Locomotion controls spatial integration in mouse visual cortex // Current Biology. 2013. 23, 10. 890–894.

Baumann Oliver, Borra Ronald J., Bower James M., Cullen Kathleen E., Habas Christophe, Ivry Richard B., Leggio Maria, Mattingley Jason B., Molinari Marco, Moulton Eric A., Paulin Michael G., Pavlova Marina A., Schmahmann Jeremy D., Sokolov Arseny A. Consensus Paper: The Role of the Cerebellum in Perceptual Processes // Cerebellum. 2015. 14, 2. 197–220.

Bernstein Jacob G., Boyden Edward S. Optogenetic tools for analyzing the neural circuits of behavior // Tre. 2011. 15, 2. 592–600.

Boele Henk Jan, Peter Saša, Ten Brinke Michiel M., Verdonschot Lucas, Ijpelaar Anna C.H., Rizopoulos Dimitris, Gao Zhenyu, Koekkoek Sebastiaan K.E., De Zeeuw Chris I. Impact of

parallel fiber to Purkinje cell long-term depression is unmasked in absence of inhibitory input // Science Advances. 2018. 4, 10. 1–9.

Bönstrup Marlene, Iturrate Iñaki, Thompson Ryan, Cruciani Gabriel, Censor Nitzan, Cohen Leonardo G. A Rapid Form of Offline Consolidation in Skill Learning // Current Biology. 2019. 29, 8. 1346–1351.e4.

Brinke Michiel M. ten, Heiney Shane A., Wang Xiaolu, Proietti-Onori Martina, Boele Henk Jan, Bakermans Jacob, Medina Javier F., Gao Zhenyu, De Zeeuw Chris I. Dynamic modulation of activity in cerebellar nuclei neurons during pavlovian eyeblink conditioning in mice // eLife. 2017. 6. 1–27.

Carey Megan R. Synaptic mechanisms of sensorimotor learning in the cerebellum // Current Opinion in Neurobiology. 2011. 21, 4. 609–615.

Chadderton Paul, Margrie Troy W., Hausser Michael. Integration of quanta in cerebellar granule cells during sensory processing // Nature. 2004. 428. 856–860.

Chettih Selmaan N., Mcdougle Samuel D., Ruffolo Luis I., Medina Javier F. Adaptive timing of motor output in the mouse: The role of movement oscillations in eyelid conditioning // Frontiers in Integrative Neuroscience. 2011. 5, November. 1–11.

Cooke Samuel F., Attwell Phillip J.E., Yeo Christopher H. Temporal Properties of Cerebellar-Dependent Memory Consolidation // Journal of Neuroscience. 2004. 24, 12. 2934–2941.

D'Angelo Egidio, Casali Stefano. Seeking a unified framework for cerebellar function and dysfunction: From circuit operations to cognition // Frontiers in Neural Circuits. 2013. 6, 116.

Dal Maso Fabien, Desormeau Bennet, Boudrias Marie Hélène, Roig Marc. Acute cardiovascular exercise promotes functional changes in cortico-motor networks during the early stages of motor memory consolidation // NeuroImage. 2018. 174, March. 380–392.

De Zeeuw Chris I., Yeo C. H. Time and tide in cerebellar memory formation // Current Opinion in Neurobiology. 2005. 15, 6. 667–674.

Dudai Yadin. The Neurobiology of Consolidations, Or, How Stable is the Engram? // Annual Review of Psychology. 2004. 55, 1. 51–86.

Dudai Yadin. The Restless Engram: Consolidations Never End // Annual Review of Neuroscience. 2012. 35, 1. 227–247.

Dudai Yadin, Karni Avi, Born Jan. The Consolidation and Transformation of Memory // Neuron. 2015. 88, 1. 20–32.

Eccles John C., Ito Masao, Szentágothai János. The Cerebellum as a Neuronal Machine. 1967.

El-Sayes Jenin, Harasym Diana, Turco Claudia V., Locke Mitchell B., Nelson Aimee J. Exercise-Induced Neuroplasticity: A Mechanistic Model and Prospects for Promoting Plasticity // Neuroscientist. 2019. 25, 1. 65–85.

Ferrer-Uris Blai, Busquets Albert, Lopez-Alonso Virginia, Fernandez-Del-Olmo Miguel, Angulo-Barroso Rosa. Enhancing consolidation of a rotational visuomotor adaptation task through acute exercise // PLoS ONE. 2017. 12, 4. 3–9.

Flourens Marie-Jean-Pierre. Recherches expérimentales sur les propriétés et les fonctions du système nerveux dans les animaux vertébrés // Crevot. 1824.

Freeman John H., Steinmetz Adam B. Neural circuitry and plasticity mechanisms underlying delay eyeblink conditioning. // Learning memory (Cold Spring Harbor, N.Y.). 2011. 18, 10. 666–677.

Fünfschilling Ursula, Reichardt Louis F. Cre-mediated recombination in Rhombic Lip Derivatives // Genesis. 2002. 33, 4. 160–169.

Galliano Elisa, Gao Zhenyu, Schonewille Martijn, Todorov Boyan, Simons Esther, Pop Andreea S., D'Angelo Egidio, Van Den Maagdenberg Arn M.J.M., Hoebeek Freek E., De Zeeuw Chris I. Silencing the Majority of Cerebellar Granule Cells Uncovers Their Essential Role in Motor Learning and Consolidation // Cell Reports. 2013. 3, 4. 1239–1251.

Garcia Keith S., Steele Philip M., Mauk Michael D. Cerebellar cortex lesions prevent acquisition of conditioned eyelid responses // Journal of Neuroscience. 1999. 19, 24. 10940–10947.

Giovannucci Andrea, Badura Aleksandra, Deverett Ben, Faezaneh Njafi, Pereira Talmo D., Gao Zhenyu, Ozden Ilker, Kloth Alexander D., Pnevmatikakis Eftychios, Paninski Liam, De Zeeuw Chris I., Medina Javier. F., Wang Samuel S.H. Cerebellar granule cells acquire a widespread

predictive feedback signal during motor learning // Nature Neuroscience. 2017. 20, 5. 727–734.

Heiney Shane A., Wohl Margot P., Chettih Selmaan N., Ruffolo Luis I., Medina Javier F. Cerebellar-dependent expression of motor learning during eyeblink conditioning in head-fixed mice // Journal of Neuroscience. 2014. 34, 45. 14845–14853.

Hesslow Germund, Svensson Pär, Ivarsson Magnus. Learned movements elicited by direct stimulation of cerebellar mossy fiber afferents // Neuron. 1999. 24, 1. 179–185.

Huang Cheng Chiu, Sugino Ken, Shima Yasuyuki, Guo Caiying, Bai Suxia, Mensh Brett D., Nelson Sacha B., Hantman Adam W. Convergence of pontine and proprioceptive streams onto multimodal cerebellar granule cells // eLife. 2013. 2013, 2. 1–17.

Ishikawa Taro, Shimuta Misa, Häuser Michael. Multimodal sensory integration in single cerebellar granule cells in vivo // eLife. 2015. 4, DECEMBER2015. 1–10.

Ito Masao. Neural Design of the Cerebellar Motor Control System // Brain Research. 1972. 40. 81–84.

Ito Masao. Control of mental activities by internal models in the cerebellum // Natue Reviews Neuroscience. 2008. 9, 4. 304–313.

Kalmbach Brian E., Ohyama Tatsuya, Mauk Michael D. Temporal patterns of inputs to cerebellum necessary and sufficient for trace eyelid conditioning // Journal of Neurophysiology. 2010. 104, 2. 627–640.

Kandel E. R. Principles of Neural Science. New York: McGraw-Hill, 2013. 5.

Kandel E. R., Dudai Yadin, Mayford Mark R. The molecular and systems biology of memory // Cell. 2014. 157, 1. 163–186.

Kassardjian Charles D., Tan Yao Fang, Chung Ji Yeon J., Heskin Raquel, Peterson Michael J., Broussard Dianne M. The site of a motor memory shifts with consolidation // Journal of Neuroscience. 2005. 25, 35. 7979–7985.

Kellett Daniel O., Fukunaga Izumi, Chen-Kubota Eva, Dean Paul, Yeo Christopher H. Memory consolidation in the cerebellar cortex // PLoS ONE. 2010. 5, 7.

Kim Jinsook, Augustine George J. Molecular Layer Interneurons: Key Elements of Cerebellar Network Computation and Behavior // Neuroscience. 2021. 462. 22–35.

Krupa David J., Thompson Judith K., Thompson Richard F. Localization of a memory trace in the mammalian brain // Science. 1993. 260, 5110. 989–991.

Lisberger Stephen G. The Rules of Cerebellar Learning: Around the Ito Hypothesis // Neuroscience. 2021. 462. 175–190.

Liu Xu, Ramirez Steve, Pang Petti T., Puryear Corey B., Govindarajan Arvind, Deisseroth Karl, Tonegawa Susumu. Optogenetic stimulation of a hippocampal engram activates fear memory recall // Nature. 2012. 484, 7394. 381–385.

Marr D. A Theory of Cerebellar Cortex // Journal of Physiology. 1969. 202. 437–470.

Martinez F. E., Crill W. E., Kennedy T. T. Electrogenesis of Cerebellar Purkinje Cell Responses in Cats // Journal of Neurophysiology. 1971. 34, 3. 348–356.

Mauk M. D., Ruiz Blenda P. Learning-Dependent Timing of Pavlovian Eyelid Responses: Differential Conditioning Using Multiple Interstimulus Intervals // Behavioral Neuroscience. 1992. 106, 4. 666–681.

Mauk M. D., Steinmetz J. E., Thompson R. F. Classical conditioning using stimulation of the inferior olive as the unconditioned stimulus. // Proceedings of the National Academy of Sciences of the United States of America. 1986. 83, 14. 5349–5353.

McCormick David A., Thompson Richard F. Cerebellum: Essential Involvement in the Classically Conditioned Eyelid Response // Science. 1984. 223. 296–299.

Medina Javier F., Garcia Keith S., Mauk Michael D. A mechanism for savings in the cerebellum // Journal of Neuroscience. 2001. 21, 11. 4081–4089.

Medina Javier F., Garcia Keith S., Nores William L., Taylor Nichole M., Mauk Michael D. Timing mechanisms in the cerebellum: Testing predictions of a large- scale computer simulation // Journal of Neuroscience. 2000a. 20, 14. 5516–5525.

Medina Javier. F., Nores W. L., Ohyama T., Mauk M. D. Mechanisms of cerebellar learning suggested by eyelid conditioning // Current Opinion in Neurobiology. 2000b. 10, 6. 717–724.

Medina Javier F., Repa J. Christopher, Mauk Michael D., LeDoux Joseph E. Parallels between cerebellum- and amygdala-dependent conditioning // Nature Reviews Neuroscience. 2002. 3, 2. 122–131.

Mittmann Wolfgang, Koch Ursula, Häusser Michael. Feed-forward inhibition shapes the spike output of cerebellar Purkinje cells // Journal of Physiology. 2005. 563, 2. 369–378.

Muzzu Tomaso, Mitolo Susanna, Gava Giuseppe P., Schultz Simon R. Encoding of locomotion kinematics in the mouse cerebellum // PLoS ONE. 2018. 13, 9. 1–26.

Niell Cristopher M., Stryker Michael P. Modulation of visual responses by behavioral state in mouse visual cortex // Neuron. 2010. 65, 4. 472–479.

Ohyama T., Mauk M. D. Latent acquisition of timed responses in cerebellar cortex // Journal of Neuroscience. 2001. 21, 2. 682–690.

Ozden Ilker, Dombeck Daniel A., Hoogland Tycho M., Tank David W., Wang Samuel S.H. Widespread state-dependent shifts in cerebellar activity in locomoting mice // PLoS ONE. 2012. 7, 8.

Perrett S. P., Ruiz B. P., Mauk M. D. Cerebellar cortex lesions disrupt learning-dependent timing of conditioned eyelid responses // Journal of Neuroscience. 1993. 13, 4. 1708–1718.

Powell Kate, Mathy Alexandre, Duguid Ian, Häusser Michael. Synaptic representation of locomotion in single cerebellar granule cells // eLife. 2015. 4, june 2015. 1–18.

Pugh Jason R., Raman Indira M. Potentiation of Mossy Fiber EPSCs in the Cerebellar Nuclei by NMDA Receptor Activation followed by Postinhibitory Rebound Current // Neuron. 2006. 51, 1. 113–123.

Ramanathan Dhakshin S., Gulati Tanuj, Ganguly Karunesh. Sleep-Dependent Reactivation of Ensembles in Motor Cortex Promotes Skill Consolidation // PLoS Biology. 2015. 13, 9. 1–25.

Raymond Jennifer L., Lisberger Stephen G., Mauk Michael D. The cerebellum: A neuronal learning machine? // Science. 1996. 272, 5265. 1126–1131.

Rescorla R. Behavioral Studies Of Pavlovian Conditioning // Annual Review of Neuroscience. 1988. 11, 1. 329–352.

Robertson Edwin M., Pascual-Leone Alvaro, Miall R. Chris. Current concepts in procedural consolidation // Nature Reviews Neuroscience. 2004. 5, 7. 576–582.

Roig Marc, Skriver Kasper, Lundbye-Jensen Jesper, Kiens Bente, Nielsen Jens Bo. A Single Bout of Exercise Improves Motor Memory // PLoS ONE. 2012. 7, 9. 28–32.

Schmahmann Jeremy D. The Cerebellar Contribution to Higher Function // Archives of Neurology. 1991. 48, 11. 1178–1187.

Schmahmann Jeremy D., Guell Xavier, Stoodley Catherine J., Halko Mark A. The Theory and Neuroscience of Cerebellar Cognition // Annual Review of Neuroscience. 2019. 42, 1. 337–364.

Shutoh F., Ohki M., Kitazawa H., Itohara S., Nagao S. Memory trace of motor learning shifts transsynaptically from cerebellar cortex to nuclei for consolidation // Neuroscience. 2006. 139, 2. 767–777.

Smith Marius C. CS-US interval and US intensity in classical conditioning of the rabbit's nictitating membrane response // Journal of Comparative and Physiological Psychology. 1968. 66, 3. 666–681.

Smith Marius C., Coleman Steven R., Gormezano I. Classical conditioning of the rabbit's nictitating membrane response at backward, simultaneous, and forward CS-US intervals // Journal of Comparative and Physiological Psychology. 1969. 69, 2. 226–231.

Smith Patrick J., Blumenthal James A., Hoffman Benson M., Cooper Harris, Strauman Timothy A., Welsh-Bohmer Kathleen, Browndyke Jeffrey N., Sherwood Andrew. Aerobic exercise and neurocognitive performance: A meta-analytic review of randomized controlled trials // Psychosomatic Medicine. 2010. 72, 3. 239–252.

Squire Larry R., Alvarez Pablo. Retrograde amnesia and memory consolidation: a neurobiological perspective // Current Opinion in Neurobiology. 1995. 5, 2. 169–177.

Squire Larry R., Dede AJ. Conscious and unconscious memory // Cold Spring Harbor Perspectives in Biology. 2015. 7, 3.

Squire Larry R., Genzel Lisa, Wixted John T., Morris Richard G. Memory consolidation // Cold Spring Harbor Perspectives in Biology. 2015. 7, 8.

Steinmetz J. E., Lavond D. G., Thompson R. F. Classical Conditioning in Rabbits Using Pontine Nucleus Stimulation as a Conditioned Stimulus and Inferior Olive Stimulation as an Unconditioned Stimulus // Synapse. 1989. 3, 3. 225–233.

Steinmetz J. E., Logan C. G., Thompson R. F. Essential involvement of mossy fibers in projecting the conditioned stimulus to the cerebellum during classical conditioning. 1988. 143–148.

Therrien Amanda S., Bastian Amy J. The cerebellum as a movement sensor // Neuroscience Letters. 2019. 688, June 2018. 37–40.

Thompson R. F., Steinmetz J. E. The role of the cerebellum in classical conditioning of discrete behavioral responses // Neuroscience. 2009. 162, 3. 732–755.

Welsh John P. Acute inactivation of the inferior olive blocks associative learning // European Journal of Neuroscience. 1998. 10, 11. 3321–3332.

Wulff Peer, Schonewille Martijn, Renzi Massimiliano, Viltono Laura, Sassoè-Pognetto Marco, Badura Aleksandra, Gao Zhenyu, Hoebeek Freek E., Van Dorp Stijn, Wisden William, Farrant Mark, De Zeeuw Chris I. Synaptic inhibition of Purkinje cells mediates consolidation of vestibulo-cerebellar motor learning // Nature Neuroscience. 2009. 12, 8. 1042–1049.

Yeo C. H., Hardiman Mervyn J., Glickstein Mitchell. Discrete lesions of the cerebellar cortex abolish the classically conditioned nictitating membrane response of the rabbit // Behavioural Brain Research. 1984. 13, 3. 261–266.

Zhang Wei, Linden David J. Long-term depression at the mossy fiber-deep cerebellar nucleus synapse // Journal of Neuroscience. 2006. 26, 26. 6935–6944.